Bioanalytical Breakthroughs:

Advanced Chromatography in Protein Analysis and Doping Detection

Article Collection

3

Contents

Cover image © Adobe Stock 895654696

Introduction

In the ever-evolving field of biomolecular analysis, the quest for precision, efficiency, and specificity has led to the development and refinement of various chromatographic techniques. They stand out as critical tools for the separation and analysis of complex biological samples. Advanced chromatography techniques, in particular, have revolutionized the way scientists approach biomolecular studies, enabling high-resolution and high-throughput analyses that were previously unattainable. They are as versatile as they are powerful, capable of tackling the separation of small metabolites to large proteins and nucleic acids.

With the advent of advanced chromatographic methods, researchers can now delve into the intricacies of biological samples with unparalleled precision. This precision is critical when it comes to the development of new pharmaceuticals, understanding metabolic pathways, and the detection of biomarkers for diseases.

One of the key aspects of advanced chromatography is its ability to maintain the integrity of the biomolecules during analysis. This is especially important for the study of intact proteins and monoclonal antibodies, where maintaining their native state is crucial for accurate characterization. Hydrophobic interaction chromatography is one such technique that has been optimized for this purpose, offering a non-denaturing environment that preserves the structure and function of these large biomolecules.

Moreover, the integration of chromatography with mass spectrometry has opened new frontiers in bioanalytical applications. The hyphenation of microflow chromatography with electrospray ionization mass spectrometry, for instance, provides a powerful tool for the analysis of low molecular weight compounds. This combination enhances sensitivity and specificity, enabling the detection of minute quantities of analytes within complex biological matrices.

In the context of sports science, advanced chromatography plays a critical role in anti-doping efforts. The detection of anabolic androgenic steroids and other performance-enhancing substances requires highly sensitive and selective analytical techniques. Chromatography, coupled with mass spectrometry, allows for the comprehensive screening and confirmation of these substances, contributing to the integrity of sports and the health of athletes.

This Article Collection compiles three pivotal research papers that underscore the significance of advanced chromatography in the analysis of biomolecules.

Each article presents a unique perspective on the application of these techniques, from setting up robust chromatographic systems to the nuances of bioanalytical approaches and the challenges of detecting doping substances in athletes.

The first article by Ewonde *et al.* (2022; **page 5-13**) offers a detailed protocol for establishing robust hydrophobic interaction chromatography tailored for analyzing intact proteins and monoclonal antibodies. The authors meticulously outline the steps for setting up the instrumentation, preparing samples, and optimizing chromatographic conditions. They demonstrate the method's effectiveness and reproducibility, highlighting its potential as a standard in protein analysis.

Girel *et al.* (2024; **page 14-34**) present a comprehensive tutorial review on the hyphenation of microflow chromatography with electrospray ionization mass spectrometry, focusing on bioanalytical applications for low molecular weight compounds. The review discusses the theoretical and practical considerations for micro-chromatography, guiding readers through the workflow and emphasizing the importance of ionization source design for enhancing sensitivity.

Lastly, the study by Börjesson *et al.* (2020; **page 36-45**) examines the biomarkers and clinical parameters in male and female users of anabolic androgenic steroids and other doping agents. The research provides insights into the substances used by athletes, the gender-specific differences in their effects, and the need for additional biomarkers, especially for female athletes. This study underscores the complexity of doping detection and the necessity for advanced chromatographic techniques in this field.

Dr. Christina Poggel
Wiley Analytical Science

A protocol for setting-up robust hydrophobic interaction chromatography targeting the analysis of intact proteins and monoclonal antibodies

Raphael Ewonde Ewonde[1] | Nico Lingg[2] | Daniel Eßer[3] | Sebastiaan Eeltink[1]

[1]Department of Chemical Engineering, Vrije Universiteit Brussel (VUB), Brussels, Belgium

[2]Department of Biotechnology, Institute of Bioprocess Science and Engineering, University of Natural Resources and Life Sciences, Vienna, Austria

[3]YMC Europe GmbH, Dinslaken, Germany

Correspondence
Sebastiaan Eeltink, Pleinlaan 2, B-1050, Brussels, Belgium.
Email: seeltink@vub.be

Abstract

Hydrophobic interaction chromatography (HIC) is a chromatographic technique that mainly targets the separation of biomolecules (intact proteins, monoclonal antibodies, etc.) based on the difference in surface hydrophobicity while applying non-denaturing conditions. This protocol paper provides guidelines for setting-up robust HIC analysis and considers the instrument configuration, mobile-phase and sample preparation, as well as chromatographic conditions and settings. The separation of a mixture of intact proteins and monoclonal antibodies is demonstrated by applying conventional HIC conditions, that is, using a mildly hydrophobic (C_4) stationary phase in combination with an inverse ammonium sulphate gradient dissolved in aqueous phosphate buffer. The effect of sample-preparation conditions on sample breakthroughs is presented. Finally, good run-to-run repeatability (relative standard deviation < 2%) is demonstrated for five different columns obtained from three different column lots, considering chromatographic retention, peak width, peak area and column pressure.

KEYWORDS
biopharmaceuticals, HPLC method development, native liquid chromatography, protein profiling

1 | INTRODUCTION TO HYDROPHOBIC INTERACTION CHROMATOGRAPHY

In 1948, Tiselius reported on a separation experiment where proteins adsorb to a stationary phase in the presence of a salt concentration that is only slightly lower concentration than is required for their precipitation.[1] It was observed that adsorption was reversible and could be mediated by the salt concentration. Tiselius referred to this technique as '*adsorption separation by salting out*', which was later renamed by Hjertén to hydrophobic interaction chromatography (HIC).[2] Similar to reversed-phase liquid chromatography, HIC separates biomacromolecules based on their hydrophobicity. However, as non-denaturing conditions are applied, the protein 3D conformation and hence biological activity is (largely) maintained.[3]

Hydrophobic interactions between analytes and the mildly hydrophobic stationary phase in an aqueous environment are driven by the change in entropy. In an aqueous environment, the stationary-phase surface and proteins containing both hydrophilic (displayed in blue) and hydrophobic (displayed in red) moieties are shielded by ordered water layers, see Figure 1A. The high ionic strength applied at the start of the gradient disrupts the ordered water layers in the immediate vicinity of the protein and the stationary-phase ligands, as salt ions are preferentially hydrated in an aqueous environment, see Figure 1B. As the entropy (ΔS) increases, while the enthalpy (ΔH)
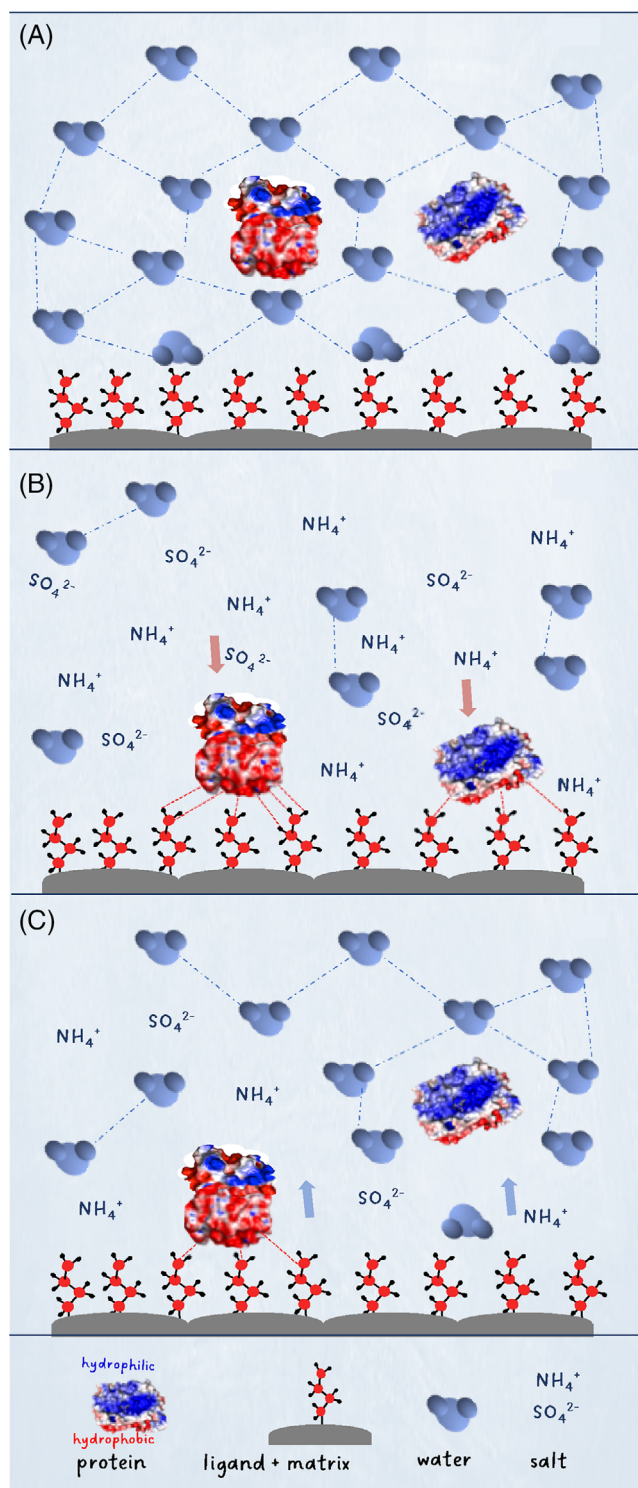
FIGURE 1 Retention mechanism for hydrophobic interaction chromatography. (A) At aqueous conditions, ordered-water layers are formed shielding the protein and stationary phase surface. (B) At high salt concentrations the ordered-water layers are disrupted, exposing hydrophobic surfaces. Proteins and stationary-phase ligands associate via hydrophobic cinteractions driven by the increase in entropy. (C) Hydrophobic interactions gradually weaken when decreasing the ionic strength of the mobile phase and proteins elute sequentially according to their surface hydrophobicity.

and temperature (T) remain constant, hydrophobic interactions are promoted by negative Gibbs free energy (ΔG),[4]

$$\Delta G = \Delta H - T \cdot \Delta S \qquad (1)$$

Proteins with more hydrophobic moieties will undergo stronger interactions with the hydrophobic stationary-phase ligands than those with more hydrophilic moieties and hence display more retention. Upon decreasing the salt concentration, the hydrophobic interactions gradually weaken as entropy is no longer a driven force. The ordered water layers are reformed, and analytes will elute in increasing order of surface hydrophobicity, see Figure 1C.

Separations based on hydrophobic interaction mediated by salt are applicable to a wide range of analytes, including some low molecular-weight analytes (<2000 Da) and (bio-)macromolecules. Considering the HIC analysis of low-molecular weight analytes (aromatic alcohol homologues, dansylamino acid) studies are merely limited to retention-time profiling while varying column chemistry and temperature.[5,6] Proof-of-concept to separate peptides and oligonucleotides with HIC has been demonstrated, albeit the achieved resolving power is currently lower compared to reversed-phase liquid chromatography (RPLC).[7,8] HIC has been extensively used for the analysis of biomacromolecules such as globular proteins, including proteoforms,[9–11] recombinant monoclonal antibodies (mAbs),[12] and antibody-drug conjugates (ADCs).[13] Critical quality attributes of ADCs that have successfully been analyzed, include the average drug-to-antibody ratio,[14] and drug-load distribution.[15] Recently, new applicability areas have been explored, including the HIC purification of viruses,[16] and the analysis of plasmids[17] and exosomes.[18]

2 | DEVELOPMENT OF THE PROTOCOL

Although HIC has been successfully applied for the analysis of a range of biomolecules, method robustness is still considered an issue. HIC involves the use of high salt concentrations and improper system care eventually leads to salt precipitation in the fluidics. Consequently, this leads to unrepeatable LC performance and ultimately irreversible column and system damage. This protocol focuses on establishing robust HIC conditions, targeting the analysis of intact proteins and monoclonal antibodies. Figure 2 shows the protocol scheme for setting-up robust HIC. Guidelines for mobile-phase and sample preparation, system configuration and conditioning are provided below. The effect of solvent composition on sample breakthrough is demonstrated. HIC analyses were performed using 4.6 × 100 mm (internal diameter [i.d.] × L) columns packed with 2.3 μm nonporous particles functionalized with butyl moieties and applying conventional elution conditions defined as an inverse linear ammonium sulfate gradient dissolved in 50 mM phosphate buffer (pH 7.0). Finally, run-to-run and column-to-column repeatability is demonstrated considering retention time, peak width and column pressure for three different column batches.
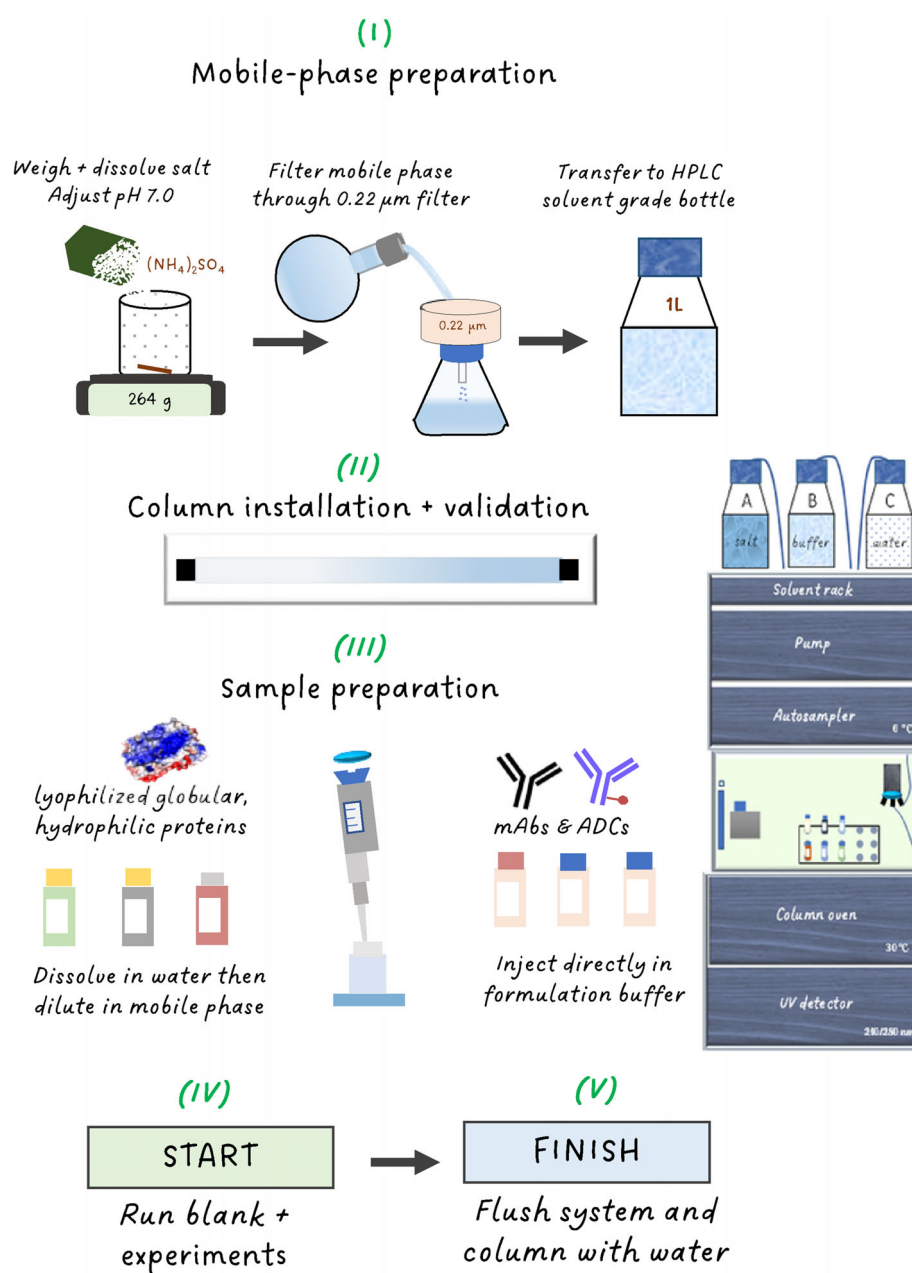
FIGURE 2 Protocol scheme for setting-up conventional analytical hydrophobic interaction chromatography.

3 | CHEMICALS AND MATERIALS

Ammonium sulfate (≥99.0%), disodium hydrogen phosphate (≥99.0%), sodium dihydrogen phosphate (≥99.0%), sodium hydroxide (high-performance liquid chromatography [HPLC] grade, 50.0%), sodium azide, myoglobin (equine heart), ribonuclease A (bovine), lysozyme (chicken egg white), trypsinogen (bovine pancreas), carbonic anhydrase (bovine erythrocytes) and α-chymotrypsinogen A (bovine pancreas) were purchased from Sigma-Aldrich (Bornem, Belgium). Monoclonal antibodies (adalimumab, trastuzumab and infliximab) were provided by BOKU (Vienna, Austria). HPLC-grade deionized water was produced in-house using a Milli-Q water purification system (Millipore, Molsheim, France).

4.6 mm i.d. × 100 mm columns packed with 2.3 μm (BioPro HIC HT) non-porous polymethacrylate particles functionalized with a butyl chemistry were obtained from (YMC Europe, Dinslaken, Germany).

4 | HPLC INSTRUMENTATION, CONFIGURATION AND MAINTENANCE

HIC experiments were conducted using an Ultimate 3000 BioRS system (Thermo Fisher Scientific, Germering, Germany) composed of a solvent rack with integrated membrane degassers, a ternary low-pressure gradient pump, a well-plate autosampler enabling in-line split-loop (flow-through needle) injections, a forced-air column oven

and a diode-array UV detector. 180 μm i.d. tubing was used to connect the pump to the injector. To maintain high separation efficiency the system was configured with 100 μm i.d. tubing between the injector and the column, and the column and the detector. The injection volume was set at 5 μL. The temperature of the well-plate sampler was set at 6°C and the column oven was maintained at 30°C. The flow rate was set at either 0.5 or 1 mL/min, see details in the figure captions. A 2.5 μL UV flow cell was used, and data was recorded at 210 and 280 nm, applying 5 Hz data collection rate and 1 s response time. Chromeleon software (version 7.2.10) was used for system control and data management.

Mobile phase A consisted of ammonium sulfate dissolved in phosphate buffer, mobile phase B consisted of phosphate buffer and mobile phase C consisted of deionized water. After installing the HIC column, the column was equilibrated with water to remove the storage solution comprising organic solvent and to prevent salt precipitation. Hereafter, the system was equilibrated first with buffer (mobile phase B) for 30 min, followed by mobile phase A for 10 min applying a flow rate of 0.5 mL/min, which corresponds to 30 and 10 column volumes, respectively. After analysis, the system and column were flushed with deionized water to remove residual salt, and the column was stored in the storage solution prescribed by the manufacturer. When the system was temporarily not in use, it was flushed with deionized water spiked with 0.05% sodium azide at a flow rate of 0.08 ml/min to prevent salt precipitation and bacteria growth in the fluidics.

Note that:

- Monitoring of the system pressure is important as an increase in system pressure may indicate salt precipitation. If the pressure increases significantly (>20 bar) it is recommended to flush the system with deionized water.
- Periodic (bi-monthly) system maintenance is advised, which includes cleaning the filter frit and flushing the system with warm water (70°C; disconnected flow cell).
- In case a significant increase in system pressure is obtained, check membrane degassers and remove salt crystals within the membrane, if any. Also, open the pump head and rinse and sonicate plungers and seals with deionized water.

5 | MOBILE-PHASE PREPARATION

Conventional HIC is performed applying a linear inverse ammonium sulfate gradient. Mobile phase A was composed of 2.3 M ammonium sulphate dissolved in 50 mM phosphate buffer pH 7.0. Mobile phase B was 50 mM aqueous phosphate buffer pH 7.0. As the addition of ions used contributes to the overall retention, it is recommended to apply the Henderson-Hasselbalch buffer formula and calculate the exact amounts of salt needed to establish the required buffer capacity and pH, while adding a minimum of sodium hydroxide in the case of a phosphate buffer to reach, for example, pH = 7.0. The recommended mobile-phase preparation is as follows:

- Add 600 ml of deionized water in a 1 L beaker and stir continuously while dissolving the weighted salts, that is, 303.60 g ammonium sulfate, 2.71 g of dibasic sodium phosphate, and 3.71 g of monobasic sodium phosphate for mobile phase A, and 2.71 g of dibasic sodium phosphate and 3.71 g of monobasic sodium phosphate for mobile phase B and add water to reach 950 ml.
- Monitor the pH with a calibrated pH meter and add 2 M aqueous NaOH solution with a dropping pipette until a pH of 7.0 is reached.
- Transfer the solution to a 1 L volumetric flask and make up to 1.0 L with deionized water.
- Filter the solutions through a 0.22 μm filter using a water jet pump, to remove microparticles and any salt clusters. Then transfer the solution to a 1 L HPLC grade solvent bottle.

Note that:

- The purity and hence color of the salt (less or more yellowish) may vary significantly between manufactures. The use of yellow ammonium sulfate impacts the UV baseline and reduces the linear detection range.
- Filtering the mobile phase reduces the pressure fluctuation and column deterioration, and hence will advance the system robustness.
- Prepared mobile phases have limited shelf time depending on the storage temperature. Typically, mobile phases are replaced every week.

6 | SAMPLE PREPARATION

In the ideal case, the sample is dissolved in the starting mobile phase to prevent sample break-through, defined as the elution of analyte at the time of an unretained analyte (t_0 time). Depending on the salt concentration and protein, precipitation may occur. To overcome this problem, the protein stock solution can be prepared in water and target salt concentration can be reached by dilution with ammonium sulfate solution (mobile phase A). The procedure is as follows:

- Weigh the appropriate mass of lyophilized sample and transfer into a clean Eppendorf tube and add deionized water to reach the protein stock concentration. Mix gently by vortexing. Protein stock solutions can be stored at -4°C in the freezer for later use.
- Dilute stock sample solution with mobile phase A to the desired concentration. It is recommended to maintain the ammonium sulphate concentration $\geq$ 50% of the starting salt concentration to achieve on-column focusing and to prevent sample break through (see discussion below).

Note that,

- Crude extracts (e.g. cell lysate) can be filtered via 0.22 μm filter membrane to remove solid microparticles.
- How long the stock sample can be stored at -4°C is protein specific. A change in chromatographic peak profile of the analyzed proteins

can be observed after prolonged sample storage (-4°C) if the protein stock solution is prepared in a concentrated salt solution instead of water.

7 | METHOD-DEVELOPMENT GUIDELINES

Figure 3 shows typical chromatograms of the separations of intact proteins that cover a wide range in hydrophobicity range applying conventional HIC conditions, that is, using a column packed with non-porous C_4 particles and applying a 15 min inverse aqueous ammonium sulfate gradient dissolved in 50 mM phosphate buffer pH 7.0. Figure 3A shows the resulting chromatogram, whereas Figure 3B shows the same separation after blank subtraction. The corresponding pressure trace is depicted in Figure 3C. In this case, the mobile phase was filtered prior to use following this protocol. When omitting mobile-phase filtration, significant pressure fluctuation is obtained, which increases over time, negatively affecting retention-time repeatability. As such, mobile-phase filtration is strongly recommended.

Most column manufacturers currently target the analysis of mAbs using C_4 column chemistry. The differences in surface coverage of C_4 chains, and therefore column hydrophobicity, affect the retention capacity, and it may be necessary to adjust the salt concentration accordingly. When analyzing highly hydrophobic macromolecules, such as some antibody-drug conjugates, either the use of a slightly more hydrophilic column can be considered, or one can use a less kosmotropic salt system, such as sodium chloride. A typical sodium chloride gradient starts at 4 M of salt. A change in column chemistry and/or salt type may result in a change in chromatographic selectivity. The addition of organic solvents to the HIC mobile phase has also been reported as an alternative approach to reduce the strength of the hydrophobic interaction.[19] It is important to realize that this may affect the 3D conformation. Our group demonstrated that the addition of only 2.5% (v/v) of IPA to the HIC mobile phase already leads to denaturation of α-lactalbumin.[20] This effect is protein specific. The addition of significant amounts of organic modifier (up to 50% [v/v]) to HIC mobile-phase systems have been reported.[21] It is questionable whether the 3D conformation and corresponding biological activity can be maintained under these conditions, and this may strongly depend on type of sample analyzed (oligonucleotides, plasmids, proteins). The elution of analytes is in this case governed by both the salt content (HIC interaction) and the amount of organic solvent (RPLC partitioning) in the mobile phase.

A large difference in the elution strength between the mobile-phase starting conditions and the sample may give rise to 'sample breakthrough', which is defined as the early elution of analytes, close to the column dead time which occurs when analytes experience (almost) no retention and hence is dissolved in a strong solvent. Figure 4 shows the separation of intact proteins while varying the ionic strength of the sample solvent. When applying a sample solution of low ionic strength, the peak area of the analytes is lower than when applying a sample solution of high ionic strength. Moreover, a breakthrough peak, marked with an asterisk, is observed, that contains proteinaceous material. Water is considered a strong solvent in HIC shielding the
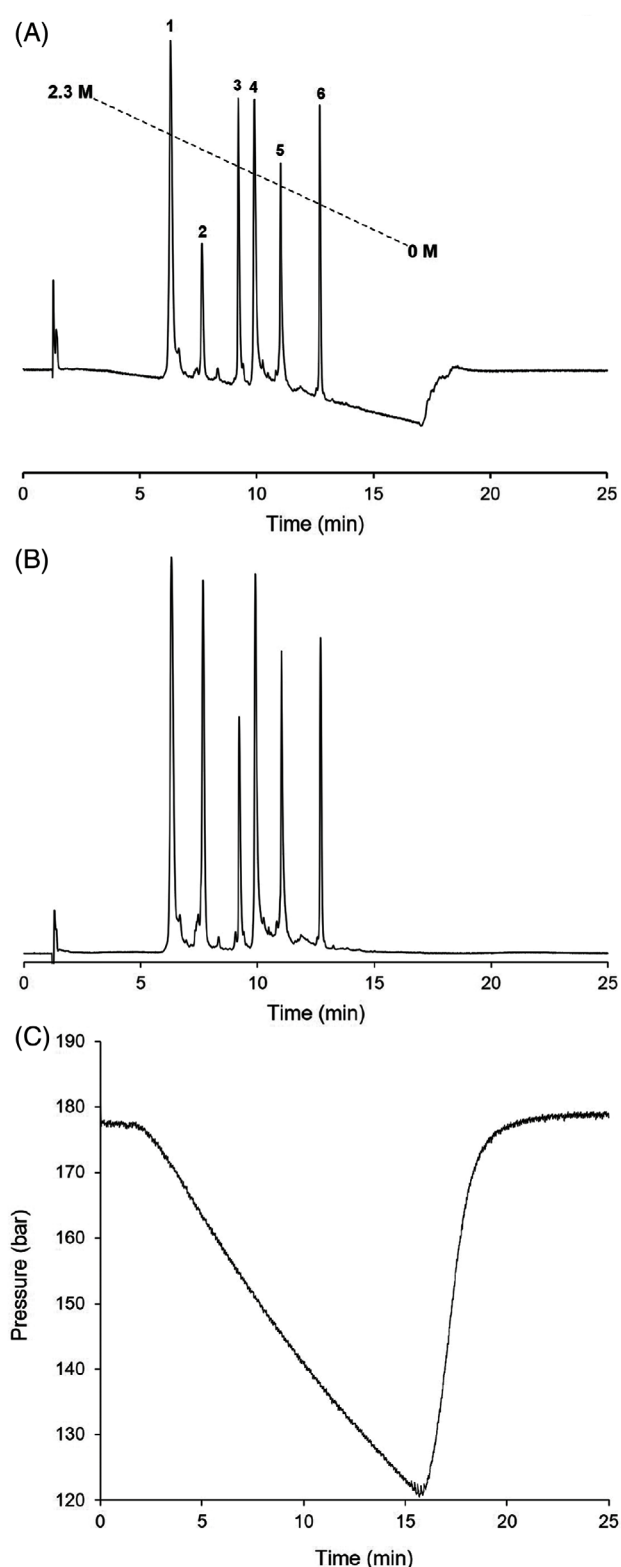
FIGURE 3 Optimized separation of a mixture of globular proteins, before (A) and after (B) blank subtraction, and the corresponding pressure profile (C). Experimental conditions: the gradient duration was 15 min and the gradient span Δc was 2.3–0 M ammonium sulfate in 50 mM phosphate buffer at pH = 7.0. Flow rate = 0.5 mL/min and the column oven was set at 30°C. Peak identification: (1) myoglobin, (2) ribonuclease A, (3) lysozyme, (4) carbonic anhydrase, (5) trypsinogen and (6) α-chymotrypsinogen A.
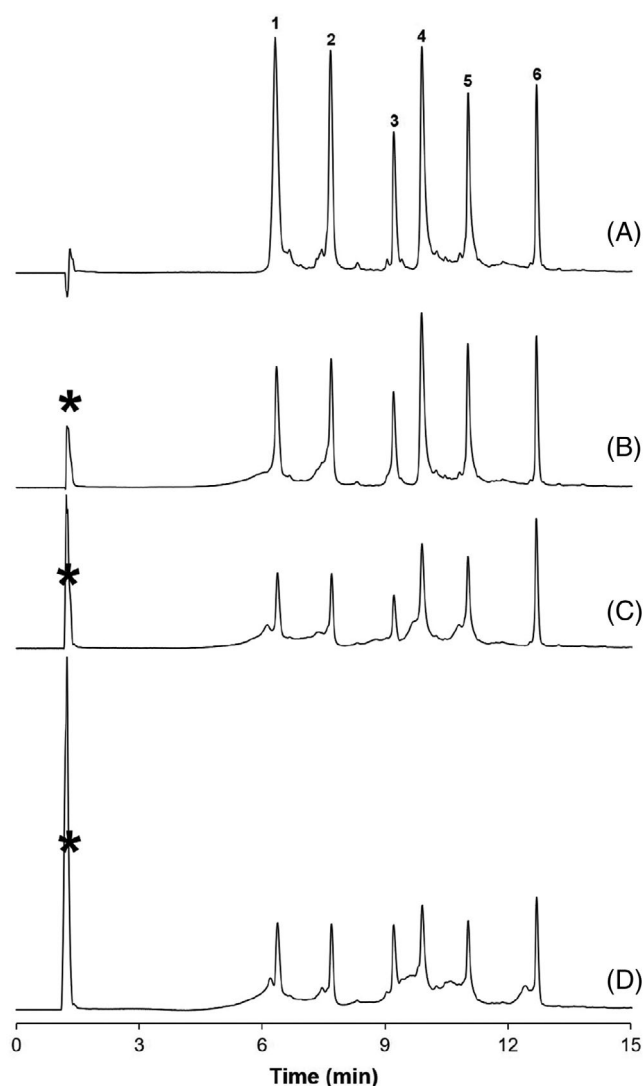
FIGURE 4 Effect of the salt concentration in the sample solution on chromatographic retention, peak profiles, and sample breakthrough (marked with an asterisk). The ammonium sulfate concentration in the sample solutions were adjusted to (A) 1.7 M, (B) 1.2 M, (C) 0.5 M and (D) 0 M. Experimental conditions and peak identification is similar as in Figure 3. The asterisk represents the sample breakthrough peak.

hydrophobic sites of the protein and preventing their interaction with the stationary phase. The mismatch between sample solvent and the mobile-phase composition compromises the accurate quantification. By increasing the ionic strength in the sample solution this problem can be circumvented.

8 | ROBUSTNESS AND COLUMN REPEATABILITY

Column robustness was assessed by measuring retention time, peak width and peak area for 30 consecutive injections applying a single column and 7.5 min ammonium sulfate gradients. Figure 5 shows the
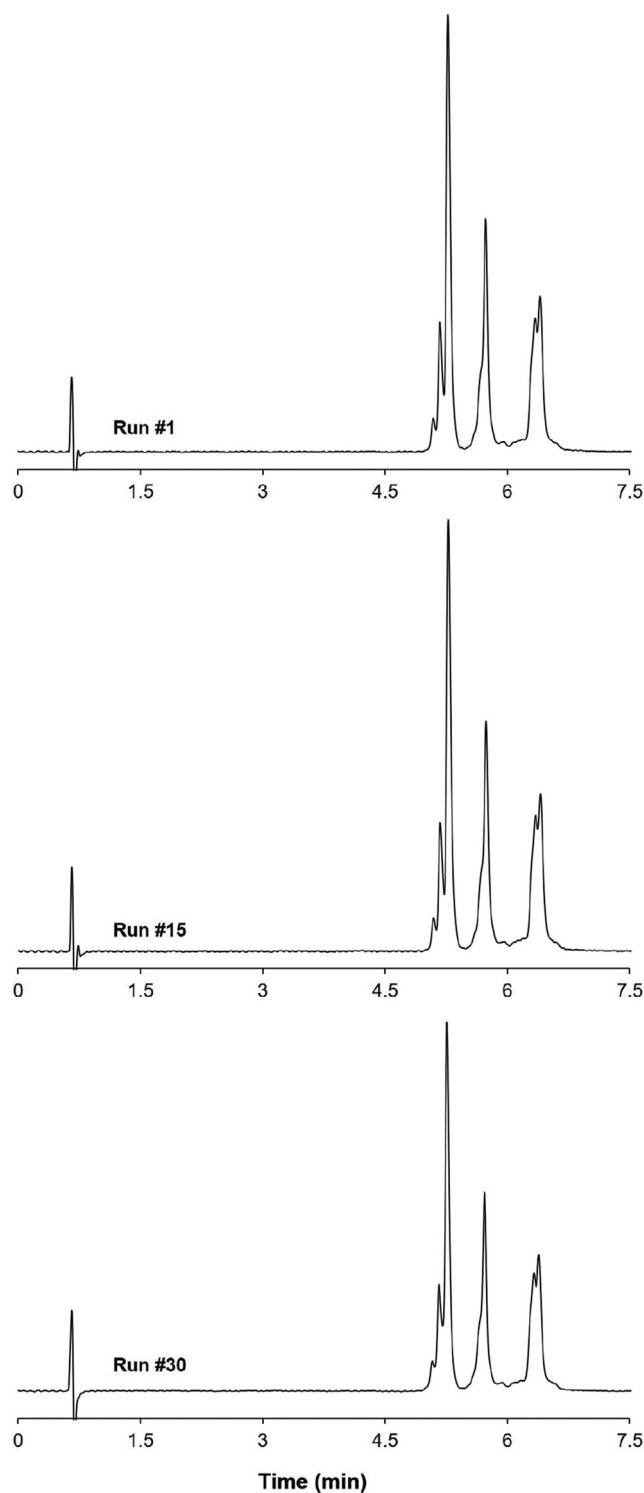
FIGURE 5 Overlay of chromatograms of a mixture of monoclonal antibodies (mAbs) demonstrating run-to-run repeatability. Experimental conditions: the gradient duration was 7.5 min and the gradient span Δc was 1.7–0 M ammonium sulfate in 50 mM phosphate buffer at pH = 7.0. Flow rate = 1 ml/min and the column oven was set at 30°C. Peak identification: (1) adalimumab, (2) trastuzumab and (3) infliximab.

TABLE 1 Run-to-run repeatability obtained for adalimumab in gradient hydrophobic interaction chromatography (HIC) mode.
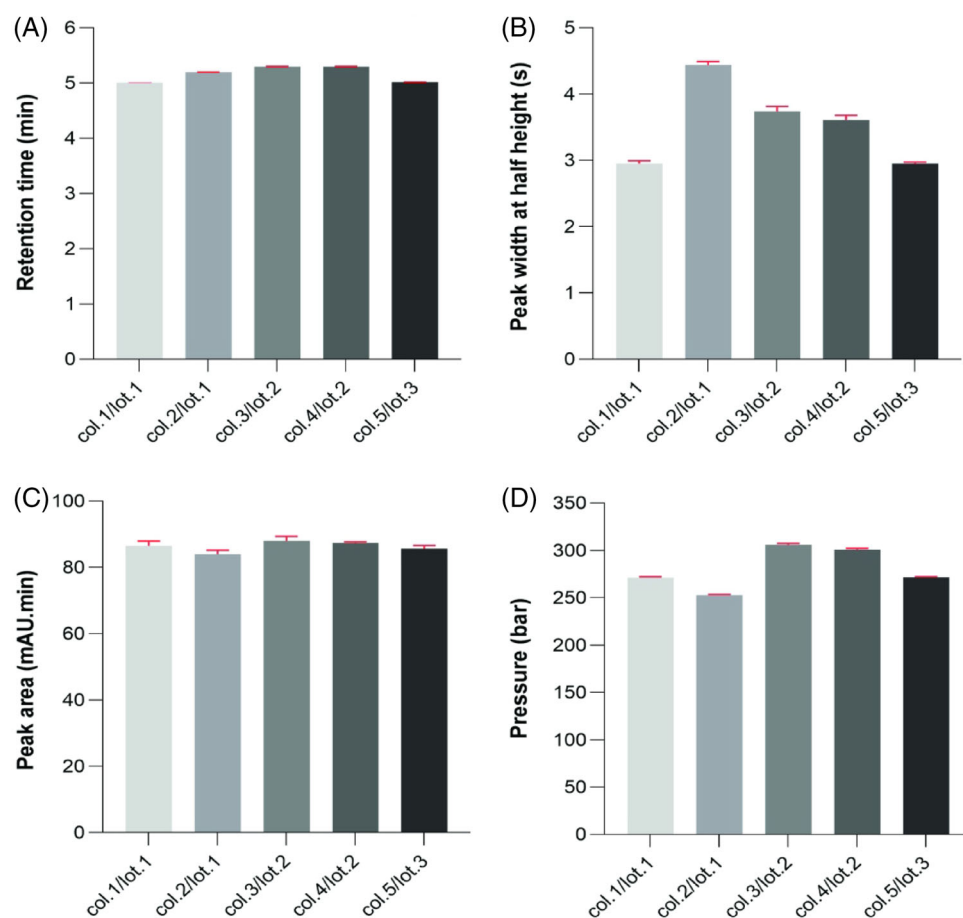
$n = 30$	Retention time (min)	Peak width at half height (s)	Peak area (mAU min)
Mean	5.272	3.26	77.06
Inferior/superior limit at 5% risk	5.270-5.277	3.24-3.330	75.97-77.15
Variance	0.000	0.00	3.45
RSD (%)	0.119	1.64	2.41

resulting overlay of blank-subtracted chromatograms (run #1, #15 and #30) of the separation of adalimumab, trastuzumab and infliximab. Statistical identical variances of retention times, peak width and peak area for adalimumab were confirmed by Fisher tests of variances, see Table 1. In a next step, the repeatability performance of five different HIC columns obtained from three different column lots was assessed following ICH guidelines, which involves comparison of six subsequent analysis runs on each column. Figure 6 depicts, for each of the columns, the corresponding mean and statistical deviation for retention time, peak width recorded at half height, peak area and column pressure

recorded at the gradient start. The relative standard deviations (RSDs) for all parameters remain small and do not exceed 2% and hence remain within the threshold set by the ICH, see Table 2 for quantitative data.

9 | CONCLUDING REMARKS

The aqueous mobile phase and neutral pH generally employed in HIC offers the possibility to maintain the 3D structure (and function) of a protein. Although the HIC conditions are considered to be mild for proteins, the high salt concentration is problematic for the HPLC instrumentation. Here, we have established a step-by-step procedure for setting up HIC for the analysis of intact proteins and monoclonal antibodies leading to robust performance. To prevent sample breakthrough, the salt concentration of the sample solvent must ideally match the gradient start composition. With the conditions established here, good run-to-run repeatability on five different columns (RSD for retention time, peak width, peak area and pressure < 2%) was achieved allowing to establish HIC for routine analysis in QC labs.

FIGURE 6 Column repeatability for different columns from three different lot numbers. Retention time, peak width and half height and peak area were determined for adalimumab. Experimental conditions are similar as stated in Figure 5.

TABLE 2 Column-to-column repeatability data obtained for five different hydrophobic interaction chromatography (HIC) columns originating from three different lots.

Column no./ lot no.		Retention time (min)	Peak width at half height (s)	Peak area (mAU min)	Pressure (bar)
1/1	Mean	5.008	2.95	86.55	271.3
	SD	0.001	0.04	1.26	0.7
	RSD	0.028	1.40	1.46	0.3
2/1	Mean	5.199	4.44	84.02	252.7
	SD	0.002	0.05	1.05	0.9
	RSD	0.029	1.10	1.25	0.4
3/2	Mean	5.016	2.95	85.70	271.8
	SD	0.002	0.02	0.83	0.4
	RSD	0.038	0.76	0.96	0.1
4/2	Mean	5.297	3.74	88.01	306.0
	SD	0.003	0.07	1.25	1.5
	RSD	0.055	1.77	1.42	0.5
5/3	Mean	5.300	3.61	87.41	300.8
	SD	0.002	0.06	0.25	1.3
	RSD	0.039	1.77	0.29	0.4

AUTHOR CONTRIBUTIONS

Raphael Ewonde Ewonde: Investigation and writing – original draft. **Nico Lingg**: Sample preparation and reviewing. **Daniel Eβer**: Conceptualization and reviewing. **Sebastiaan Eeltink**: Funding acquisition, conceptualization, writing, review & editing and supervision.

ACKNOWLEDGEMENTS

CONFLICT OF INTEREST
VUB and BOKU authors declare that they have no conflict in interest. Sebastiaan Eeltink is Editor-in-Chief of Analytical Science Advances. Daniel Eβer is an employee of YMC Europe.

DATA AVAILABILITY STATEMENT
The data that support the findings of this study are available from the corresponding author upon reasonable request.

REFERENCES
1. Tiselius A. Adsorption separation by salting out. *Ark Kemi Mineral och Geol B*. 1948;26(1).
2. Hjertén S. Some general aspects of hydrophobic interaction chromatography. *J Chromatogr A*. 1973;87(2):325-331. 10.1016/S0021-9673(01)91733-9
3. Fausnaugh JL, Pfannkoch E, Gupta S, Regnier FE. High-performance hydrophobic interaction chromatography of proteins. *Anal Biochem*. 1984;137(2):464-472. 10.1016/0003-2697(84)90114-3
4. Queiroz JA, Tomaz CT, Cabral JMS. Hydrophobic interaction chromatography of proteins. *J Biotechnol*. 2001;87(2):143-159. 10.1016/S0168-1656(01)00237-1
5. Wei Y, Yao C, Zhao J, Geng X. Influences of the mobile phase composition and temperature on the retention behavior of aromatic alcohol homologues in hydrophobic interaction chromatography. *Chromatographia*. 2002;55(11):659-665. 10.1007/BF02491779
6. Haidacher D, Vailaya A, Horváth C. Temperature effects in hydrophobic interaction chromatography. *Proc Natl Acad Sci U S A*. 1996;93(6):2290. 10.1073/PNAS.93.6.2290
7. Bobály B, Fleury-Souverain S, Beck A, Veuthey JL, Guillarme D, Fekete S. Current possibilities of liquid chromatography for the characterization of antibody-drug conjugates. *J Pharm Biomed Anal*. 2018;147:493-505. 10.1016/j.jpba.2017.06.022
8. Diogo MM, Queiroz JA, Prazeres DMF. Hydrophobic interaction chromatography of homo-oligonucleotides on derivatized sepharose CL-6B application of the solvophobic theory. *J Chromatogr A*. 2002;944(1-2):119-128. 10.1016/S0021-9673(01)01388-7
9. Zhang S, Zhang L, Jiao Y, et al. Lactobacillus delbrueckii subsp. bulgaricus proteinase: purification by ion-exchange and hydrophobic interaction chromatography. *Int J Food Prop*. 2015;18(7):1560-1567. 10.1080/10942912.2014.921199
10. Velkov T, Lim MLR, Capuano B, Prankerd R. A protocol for the combined sub-fractionation and delipidation of lipid binding proteins using hydrophobic interaction chromatography. *J Chromatogr B Anal Technol Biomed Life Sci*. 2008;867(2):238-246. 10.1016/j.jchromb.2008.04.011
11. Santos MJ, Teixeira JA, Rodrigues LR. Fractionation and recovery of whey proteins by hydrophobic interaction chromatography. *J Chromatogr B Anal Technol Biomed Life Sci*. 2011;879(7-8):475-479. 10.1016/j.jchromb.2011.01.003
12. Boyd D, Kaschak T, Yan B. HIC resolution of an IgG1 with an oxidized Trp in a complementarity determining region. *J Chromatogr B Anal Technol Biomed Life Sci*. 2011;879(13-14):955-960. 10.1016/j.jchromb.2011.03.006
13. Fekete S, Veuthey JL, Beck A, Guillarme D. Hydrophobic interaction chromatography for the characterization of monoclonal antibodies

and related products. *J Pharm Biomed Anal*. 2016;130:3-18. 10.1016/j.jpba.2016.04.004

14. Matsuda Y, Mendelsohn BA. Recent advances in drug–antibody ratio determination of antibody–drug conjugates. *Chem Pharm Bull.* 2021;69(10):976-983. 10.1248/CPB.C21-00258

15. Sun MMC, Beam KS, Cerveny CG, et al. Reduction-alkylation strategies for the modification of specific monoclonal antibody bisulfides. *Bioconjug Chem.* 2005;16(5):1282-1290. 10.1021/BC050201Y/SUPPL_FILE/BC050201YSI20050817_112445.PDF

16. Weigel T, Soliman R, Wolff MW, Reichl U. Hydrophobic-interaction chromatography for purification of influenza A and B virus. *J Chromatogr B*. 2019;1117:103-117. 10.1016/j.jchromb.2019.03.037

17. Moreira KA, Diogo M, Prazeres DM, De Lima Filho JL, Figueiredo Porto AL. Purification of plasmid (pVaxLacZ) by hydrophobic interaction chromatography. *Braz Arch Biol Technol.* 2005;48:113-117. 10.1590/s1516-89132005000400014

18. Huang S, Wang L, Bruce TF, Marcus RK. Isolation and quantification of human urinary exosomes by hydrophobic interaction chromatography on a polyester capillary-channeled polymer fiber stationary phase. *Anal Bioanal Chem.* 2019;411(25):6591-6601. 10.1007/s00216-019-02022-7

19. McCue JT. Theory and use of hydrophobic interaction chromatography in protein purification applications. *Methods Enzymol.* 2009;463(C):405-414. 10.1016/S0076-6879(09)63025-1

20. Baca M, De Vos J, Bruylants G, et al. A comprehensive study to protein retention in hydrophobic interaction chromatography. *J Chromatogr B.* 2016;1032:182-188. 10.1016/j.jchromb.2016.05.012

21. Chen B, Peng Y, Valeja SG, Xiu L, Alpert AJ, Ge Y. On-line hydrophobic interaction chromatography-mass spectrometry for top-down proteomics. *Anal Chem.* 2016;88(3):1885-1891. 10.1021/acs.analchem.5b04285

Hyphenation of microflow chromatography with electrospray ionization mass spectrometry for bioanalytical applications focusing on low molecular weight compounds: A tutorial review

Sergey Girel[1] 🆔 | Isabel Meister[1,2] | Gaetan Glauser[3] | Serge Rudaz[1,2]

[1]Institute of Pharmaceutical Sciences of Western Switzerland, University of Geneva, Geneva, Switzerland

[2]Swiss Center of Applied Human Toxicology (SCAHT), Basel, Switzerland

[3]Neuchâtel Platform of Analytical Chemistry, University of Neuchâtel, Neuchâtel, Switzerland

Correspondence
Serge Rudaz, Institute of Pharmaceutical Sciences of Western Switzerland, University of Geneva, Geneva 4, Switzerland.
Email: serge.rudaz@unige.ch

Abstract

Benefits of miniaturized chromatography with various detection modes, such as increased sensitivity, chromatographic efficiency, and speed, were recognized nearly 50 years ago. Over the past two decades, this approach has experienced rapid growth, driven by the emergence of mass spectrometry applications serving -omics sciences and the need for analyzing minute volumes of precious samples with ever higher sensitivity. While nanoscale liquid chromatography (flow rates $<1\,\mu\text{L/min}$) has gained widespread recognition in proteomics, the adoption of microscale setups (flow rates ranging from 1 to $100\,\mu\text{L/min}$) for low molecular weight compound applications, including metabolomics, has been surprisingly slow, despite the inherent advantages of the approach. Highly heterogeneous matrices and chemical structures accompanied by a relative lack of options for both selective sample preparation and user-friendly equipment are usually reported as major hindrances. To facilitate the wider implementation of microscale analyses, we present here a comprehensive tutorial encompassing important theoretical and practical considerations. We provide fundamental principles in micro-chromatography and guide the reader through the main elements of a microflow workflow, from LC pumps to ionization devices. Finally, based on both our literature overview and experience, illustrated by some in-house data, we highlight the critical importance of the ionization source design and its careful optimization to achieve significant sensitivity improvement.

KEYWORDS
bioanalysis, electrospray, mass spectrometry, microflow chromatography

1 | INTRODUCTION

Electrospray ionization mass spectrometry (ESI-MS) is widely recognized in modern bioanalytical science as a key tool supporting drug discovery, biomarker research, routine clinical diagnostics and forensic investigations (Gika et al., 2014; Kahl et al., 2019; Olesti et al., 2021; Shipkova & Svinarov, 2016). The robust performance of ESI-MS enables a highly sensitive and selective detection method for the characterization of thousands of ionized

molecules based on their mass-to-charge (*m/z*) ratios and fragmentation patterns. Recent advances in automation, instrument design and software development have significantly enhanced the user friendliness of the technique, enabling stable operation by relatively little experienced personnel, for example, in point-of-care testing (Fedick et al., 2017). This development is particularly noteworthy as mass spectrometry increasingly plays a pivotal role in personalized medicine approaches, allowing for a comprehensive exploration of a patient's chemical phenotype to deliver customized solutions. The integration of machine learning algorithms further improves the practical utility of the resulting data, transforming it from a mere readout on several biomarkers to a specific disease pattern with higher predictive power (Banerjee, 2020; Clarke, 2016).

Hyphenation of liquid chromatography (LC) adds an orthogonal separation dimension, as the analytes are sorted before the MS inlet according to their mode of interaction with mobile and stationary phases. The resulting multidimensional datasets are further enriched with information on isomeric and isobaric analytes, which are often indistinguishable by their *m/z* ratios and/or fragmentation patterns. A plethora of LC condi-tions can be found in terms of selectivity, chromato-graphic resolution, analysis speed and sensitivity (Gika et al., 2014; Harrieder et al., 2022). However, the choice of the LC setup for a particular analytical workflow should be carefully considered as MS becomes a cornerstone in the analytical process due to its costs and functionalities involved. The majority of current LC/ESI-MS applications use mobile phase flow rates between 200 μL and 1 mL/min with narrow bore analytical columns of internal diameters (ID) between 2.1 and 4.6 mm. These columns are typically connected to pneumatically assisted heated ionization sources present in nearly every MS instrument (Plumb et al., 1999; Van Dongen & Niessen, 2012; Want et al., 2013). Such setup effectively nebulizes the effluent, allowing these wide-spread platforms to generate reliable data on relatively abundant and/or easy-to-ionize analytes, with high throughput (typically 2–10 samples per hour). By contrast, detection of very low abundant analytes (pM or low nM) in complex biological matrices, or those exhibiting lower stability or ionization efficiency, still requires a considerable effort in this setting (Aubry, 2011; Li et al., 2021).

Miniaturized LC systems with nanoflow chromatography and electrospray regimes have historically dominated certain fields such as bottom-up proteomics (Ishihama, 2005; Prabhu et al., 2020). With such set ups, the introduction of peptides into the MS inlet at a flow rate of 50–1000 nL/min leads to a remarkable increase in ion generation—up to 500 times more ions than with classic chromatography. Notably, efficient bottom-up proteomics methods have been recently reported even at higher flow rates of up to 50 μL/min). This approach prioritizes system robustness and through-put, albeit at the expense of sensitivity and proteome coverage (Bian et al., 2020). In this work, we focus on the relatively unexplored field of microflow applications dedicated to low molecular weight compounds (LMWC). LMWC are characterized by a molecular weight below 1500 Da, a high degree of structural heterogeneity and, consequently, an absence of common behaviour in terms of ionization efficiencies and fragmentation patterns. This distinguishes them from proteolytic peptides and lipids (Figure 1).

To measure these more complex and highly heterogeneous analytes in various matrices requires a diversity of sample preparation protocols and chromatographic strategies compared to typical bottom-up proteomics or lipidomics analyses. The need to concentrate low quantities of analytes from large amounts of sample increases the probability to damage the fragile flow path of microscale systems, such as valves, fittings and electrospray emitters, via precipitation and/or clogging (Chetwynd & David, 2018; Desmet & Eeltink, 2013). Despite these challenges, low flow techniques overall provide great benefits when hyphenated to ESI-MS detector, and bioanalytical applications featuring a wide variety of LMWC are slowly gaining momentum, thanks to the increasing availability of diverse sample preparation methods, microcolumns and user-friendly instrumentation. This work aims to present an illustrative guide for those interested in the implementation of LC/ESI-MS bioanalytical methods tailored for LMWC using flow rates from 1 to 100 μL/min.

2 | MINIATURIZED LC/ESI-MS: THEORETICAL CONSIDERATIONS

The emergence of MS-based metabolomics and proteomics in the early 2000s sparked renewed interest in low flow setups within the scientific community. In these fields of application, sample availability is often limited to a few μL, necessitating the adoption of microfluidic approaches throughout the entire analysis. This is because the reduction in column ID increases sample peak concentration, expressed as $C_{max} = mN^{1/2}/(2\pi^{1/2}) \cdot V_0(1 + k)$ where m is the absolute mass load of the analyte at retention factor k on a column with efficiency N and dead volume V_0 (Abian et al., 1999). Therefore, a constant mass load with a reduction in column ID from 2.1 to 0.3 mm can result in an approximately 40-fold
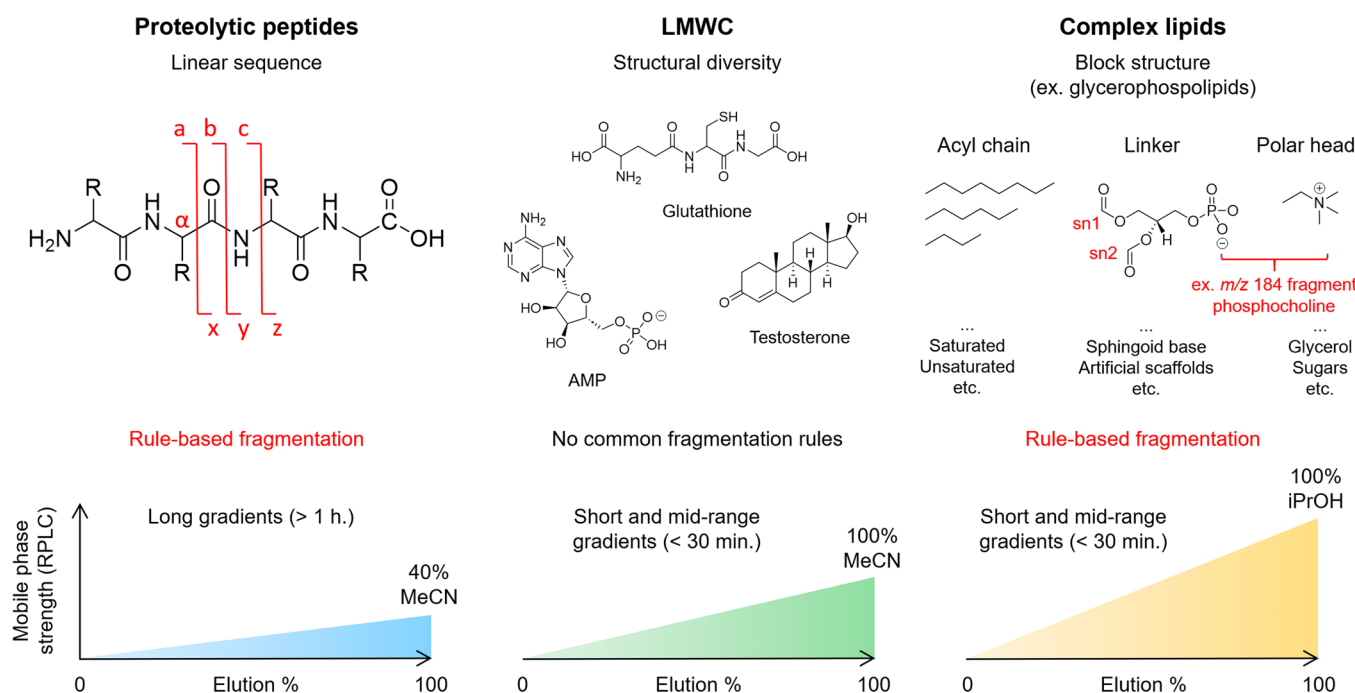
FIGURE 1 Global comparison between proteolytic peptides, low molecular weight compounds and complex lipids concerning their mass-spectrometric and reversed-phase liquid chromatography behaviors. [Color figure can be viewed at wileyonlinelibrary.com]

increase in C_{max}. To maintain identical chromatographic performances, the reduction of column diameter inherently leads to a decrease in injection volume and in the corresponding peak volumes of the separated analytes. These statements, however, hold true only if the analyte of interest is located at the column head after injection as a narrow band (e.g., without overloading, splitting, diffusion, and so forth; see Section 3.3 for considerations on injection volumes). The optimal detector volume, in this context, should not exceed one peak standard deviation σ_V. This relationship is defined by the equation $\sigma_V = V_{col} \cdot (1 + k')/N^{1/2}$, where V_{col} represents the column volume, N is the column efficiency in isocratic mode, and k' is the apparent retention factor (Desmet & Eeltink, 2013). As ion transport, mass analysis and detection in a mass spectrometer proceed on a different time scale (ms to μs) compared to chromatographic elution (s), this requirement is satisfied for LC/ESI-MS (Spaggiari et al., 2013; Vanderlinden et al., 2016). How-ever, mass spectrometers produce analytically useful (e.g., suitable for quantitation) signal based on mass flow, specifically the absolute number of ions hitting the detector. In theory, it should inevitably lead to a lower signal-to-noise ratio as the number of analyte ions is limited by a very small amount of injected material (Desmet & Eeltink, 2013; Poppe, 1997). From this perspective, chromatographic miniaturization alone may not necessarily yield the desired sensitivity increase, as the gain in analyte peak concentration is undermined

by a decrease in flow. This behavior is typically observed at very low flow rates (generally <100 nL/min) (Abian et al., 1999; Bonvin et al., 2012; Marginean et al., 2008). In practice, a decrease in flow rate demonstrates an opposite effect for ESI/MS, dramatically increasing the available signal. This phenomenon is rooted in different efficiencies of ion production and sampling associated with various ionization source designs and chemical properties of the analytes.

2.1 | Electrospray in low-flow regime

An enhanced ESI response and following sensitivity gains depend both on the ion source design and the chemical nature of the analyte resulting in different ionization efficiencies. Emitters of low-flow ion sources are usually placed closer to MS inlet, thus expanding the part of the captured ESI plume. In addition, the diameter of the emitting capillary is reduced to stabilize the Taylor cone at lower flow rates. Consequently, reduced emitter dimensions facilitate the production of smaller droplets with a higher surface-to-volume ratio, enhancing the desolvation process and increasing the charge available to analytes (Maxwell et al., 2010; Reschke & Timperman, 2011; Yuill et al., 2013). The combination of improved ion sampling and enhanced ion generation significantly impacts the performance of the ionization source: for conventional interfaces only 1 out of 2×10^5

analyte ions are typically detected by the MS detector. In contrast, nano-ESI improves this ratio to 1/400, resulting in a 500-fold better signal (Abian et al., 1999; Plumb et al., 1999). Actually, it is even possible to achieve sampling efficiencies close to 100%, using nanoflow regime and modification of standard ion optics. However, this is still not the case for microflow and analytical interfaces (Schneider et al., 2021).

The observed sensitivity gains in low flow regime may greatly vary between different analytes. It is therefore essential to briefly understand physico-chemical consider-ations at play. Differences in ESI efficiency between molecules are primarily dictated by polarity, which determine its position within the charged droplets in the spray (Enke, 1997). Less polar analytes have a stronger affinity to the highly charged droplet surface, while solvophilic species preferably reside in the droplet interior (Gomez & Tang, 1994). Consequently, the failure to migrate to the surface and participate to the excess charge will translate to a lack of ESI response. As an example, peptides with the most hydrophobic side chains will usually display higher ESI responses compared to those containing less hydrophobic motifs (Cech & Enke, 2000; Liang & Paul, 1993). Interested readers can consult literature on ion production mechanisms in ESI in detail elsewhere (Cech & Enke, 2001; Konermann et al., 2013).

In the particular case of bioanalytical applications, mixtures of analytes with different physico-chemical properties are frequent, leading to an increased competi-tion for the droplet periphery. Phospholipid species (and complex lipids in general), a typical interferent in biofluids or tissues, provide an excellent example. They usually display a high ionization efficiency and tend to outcompete other analytes at the droplet surface. It is thus expected that a low flow regimen will not dramatically enhance their ionization. In contrast, it may simply diminish their capacity to interfere at ionization with other coeluting molecules in the same polarity range, such as steroids or endocannabinoids. For instance, Danne-Rasche et al. showed that employment of nanoflow in lipidomic analysis was able to enhance the ionization of low abundant co-eluting isomers, increasing the total number of identified lipid species up to a factor 4 compared to conventional UHPLC methods (Danne-Rasche et al., 2018). On the other hand, solvophilic analytes, such as glycosides, would also greatly benefit from low flow approaches. Nanoflow has indeed proven essential for the measurement of underivatized neutral oligosaccharides in ESI-MS. Bahr and colleagues demonstrated a better ionization of maltopentose in nanoflow conditions, where competition with peptides for the droplet surface was diminished (Bahr et al., 1997; Karas et al., 2000).

## 2.2 | Categorization of microflow setups

In general, the commonly used approach to categorize LC/ESI-MS setups is solely based on column ID (Bian et al., 2022; Saito et al., 2004). Here, we prefer to emphasize flow rates, which share a strong relationship with the electrospray capillary ID to obtain maximum sample utilization efficiency (Bonvin et al., 2012). Flow rate serves as an immediate indicator for the expected signal improvement of the method under development compared to the established approaches (Figure 2).

From Figure 2, it becomes immediately clear that while the notions of robustness and throughput bear a certain degree of correlation and are proportional to the flow rate, they come at the expense of sensitivity. The primary impact on robustness at lower flow rates stems from reduced IDs of columns, liquid connections and emitter in the sample flow path, more prone to clogging and damage (Hilhorst et al., 2014). Throughput in turn depends on a careful management of extra-column volumes in the system, such as injectors, valves and fluidic connections, which can significantly impact the run time (Desmet & Eeltink, 2013). We argue that microflow regimes may represent the best compromises in terms of overall performances by providing a strategic combination of high throughput and sensitivity with acceptable robustness. Moreover, any apparent lack of robustness can be offset by a scrutinized development of sample preparation protocols and by following the equipment operating procedures.

3 | TECHNICAL DETAILS OF MINIATURIZED LC SYSTEMS FOR ESI-MS

3.1 | Mobile phase delivery

Accurate, reproducible, stable and pulse-free low flow is imperative for the functionality of microscale LC/ESI-MS setup. Such flow can be generated using various devices, operating in either constant pressure or constant flow modes. Today, the predominant choice for commercially available user-friendly systems involves piston-based binary pumps coupled with a flow controller. In these setups, the flow controller constantly measures actual outputs at the outlet of the pumps plus the total flow rate and establishes a feedback loop for a precise piston motion control, ensuring a stable flow down to the nL/min range. In typical microflow working conditions, between 5 and 30 μL/min for column diameters of 0.3 and 0.5 mm, the resulting smallest flow to be delivered by one pump will vary from 0.25 to 1.5 μL/min, considering
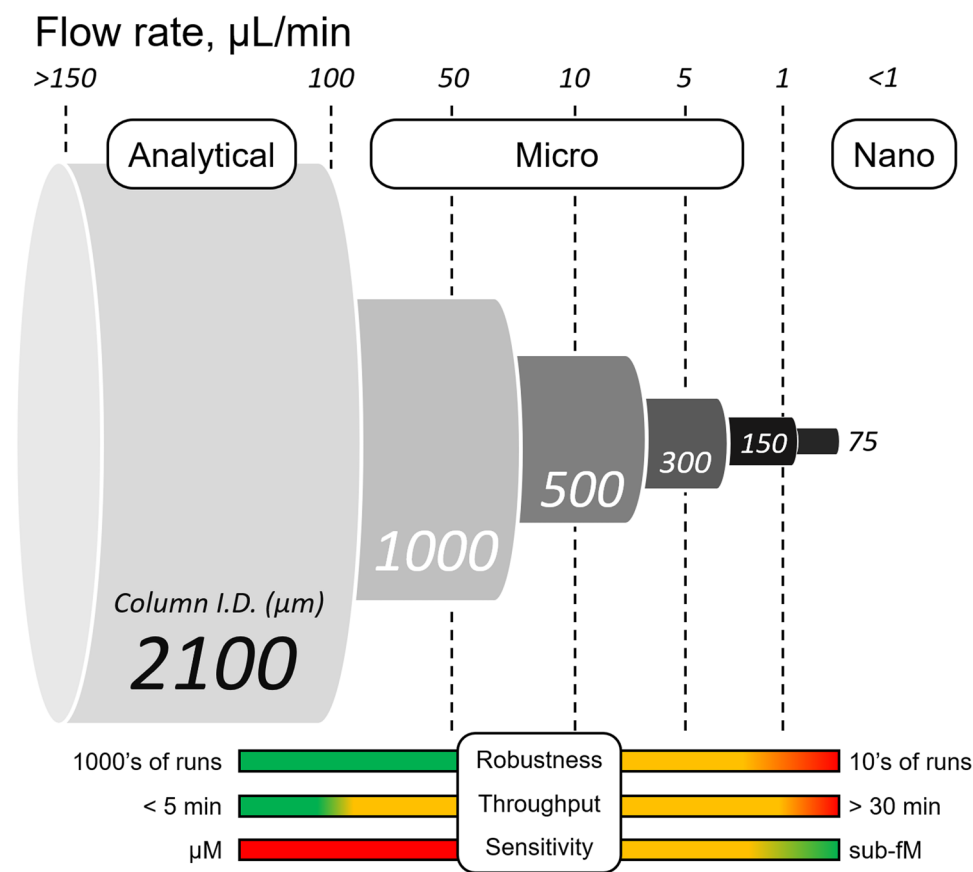
FIGURE 2 Fundamental assumptions regarding the robustness, throughput and sensitivity of liquid chromatography/electrospray ionization mass spectrometry setups considering the different flow rates range with column dimensions. [Color figure can be viewed at wileyonlinelibrary.com]

5% of strong mobile phase at the run start. The combination of binary pumps with an active flow controller is thus crucial to deliver robust gradients (Figure 3). In addition, the delay volume of these pumps is extremely reduced to avoid excessive method runtime and loss of chromatographic resolution. Table 1 provides a concise overview of the technical specifications for some commercially available systems designed for microflow applications. Additional details, including the technical specifications of discontinued, but still widely used microflow chromatographs, as well as emerging technologies, can be found elsewhere (Nazario et al., 2015; Šesták et al., 2015).

3.2 | Fluidic connections

The impact of band broadening is critical when working at low flow rates and should be minimized to the greatest extent possible. Band broadening can be expressed in terms of variance as a sum of contributions from various parts of the setup such as $\sigma^2_{tot} = \sigma^2_{column} + \sigma^2_{injector} + \sigma^2_{tubing} + \sigma^2_{detector}$ (Deridder et al., 2018; Desmet & Eeltink, 2013; Prüß et al., 2003). In case of gradient elution, the primary significant term is σ^2_{tubing}, and more specifically the tubing located between the column and mass detector (including the electrospray capillary). It can be calculated using Taylor-Aris equation as $\sigma^2_{tubing} = r^4 l\pi F/384 \cdot D_m$, where r and l represent the radius and length of capillary, F is the flow rate and D_m is the diffusion constant of the analyte in the mobile phase (Bello et al., 1994). Contributions from precolumn volume are effectively eliminated by gradient focusing effects (see Ch. 3.3), while mass spectrometric detection exerts no influence as ion transfer times from the inlet to detector proceed on a different timescale as outlined in Ch. 2.

Originally, establishing reliable fluidic connections posed a significant challenge in adopting microflow, requiring skilled operators to manually produce polished fused silica capillaries of required dimensions. Nowadays, various suppliers offer prefabricated fittings, ensuring leak-free connections and effectively eliminating connectivity issues. Table 2 provides a summary of
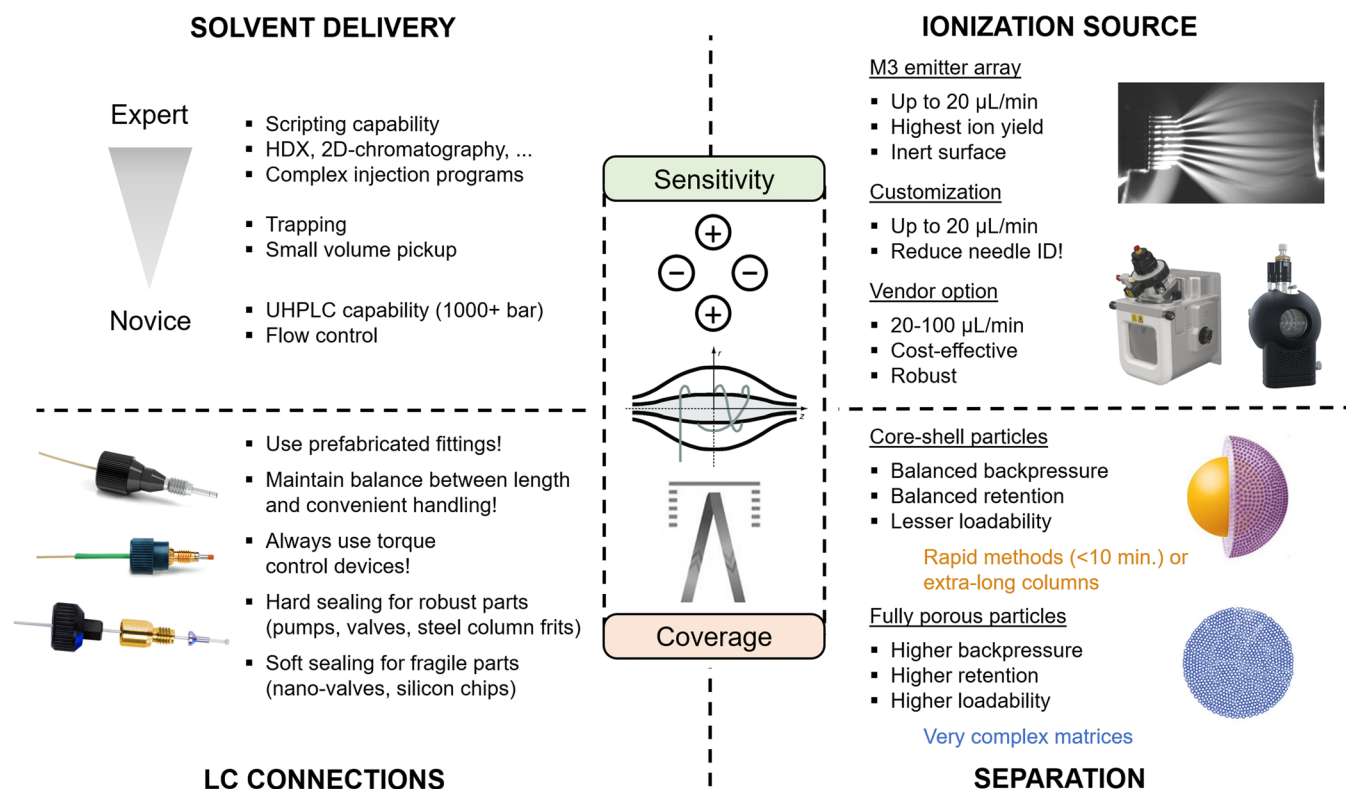
FIGURE 3 A graphical summary of the important hardware features to consider when planning microflow experiments. [Color figure can be viewed at wileyonlinelibrary.com]

TABLE 1 Technical specifications of currently marketed pumping systems for μLC/ESI-MS from major vendors.

Vendor	Thermo Fisher	Waters	Sciex	Shimadzu	Bruker
Brand	Vanquish Neo	M-Class	M5 MicroLC	Nexera Mikros	NanoElute 2
Design	Serial dual piston	Serial linear drive (2x)	Air pressure	Serial piston	Syringe
Gradient delivery	Binary				
Flow rate, μL/min	0.01–200	0.2–100	1–200	1–500	0.05–2
Active flow control	Yes	Yes	Yes	No	Yes
Pressure limit, bar	1500	1000	690	800	1000
Operating pH	2–10	2–10	1–10	2–10	2–10
Solvent degassing	Wash	Wash, A2/B2 channels	n/a	Separate module	n/a
Delay volume	<0.5 μL	<2 μL	<3 μL	<2 μL	<2 μL
Flow precision calibration	Yes	Yes	No	No	Yes

currently available fittings to connect the components of microflow setups in the established 1/16″ (10/32 thread) format. To prolong the life of equipment and ensure reproducibility of the fluidic connections, it is strongly advised to use torque control while creating the connection. In our experience, 0.35–0.4 Nm torque wrench works well with nanoVipers and Waters ZenFit connectors, requiring only the head piece to be produced independently by creating a slit for the capillary in a bar with a column head geometry. We however advise against using Marvel XAct fittings with embedded torque control on fragile parts such as silicon chips or nano-valves. Of note, a rather strong effort is required with hard PEEK sealings to produce a haptic response and leak-free connection (Figure 3). Finally, it is worth keeping attention to which materials are used for needles, flow path, valves and other parts coming in contact with the analytes to avoid nonspecific adsorption.

TABLE 2 Prefabricated fittings for user-friendly fluidic connections of μLC/ESI-MS setups from major vendors.

Vendor	Thermo Scientific	Waters	IDEX
Brand	nanoViper	ZenFit	Marvel XACT[a]
Sealing	Soft PEEK[b]	Vespel	PEEK
Material, μm ID	PEEKSil[c] 20, 50, 75 100 MP35N 100	PEEKSil 25, 40, 75, 100	PEEKSil 25, 50, 75, 100 PEEK-lined stainless steel 25, 50, 75, 100
Length, mm	150, 250, 350, 500, 750, 1000	250, 500, 650, 750, 1500	100, 150, 300, 500, 750, 1000
Backpressure, bar	1200, 1500	1000	1300
Fingertight	Yes	Yes	Yes
Torque limiting	Wrench[d]	Wrench[d]	Yes
pH range	1–10	1–10	1–10

[a]Same fittings are offered by Phenomenex as SecurityLink™ and Bruker for fluidic connections of NanoElute LC devices.

[b]Polyether etherketone.

[c]PEEK-lined fused silica.

[d]Available from Thermo, 3rd party LC/MS equipment vendors or to be produced in-house.

In most cases, MP35N and PEEKsil will be sufficient. The latter is also used to build prefabricated fittings of suitable IDs, which should be used to connect all the parts of the setup.

In practice, it is essential to keep the ID and length of the tubing as small as possible for the available backpressure. All connections should be made using zero dead volume (ZDV) connectors. Typically, 25 μm ID capillaries are suitable for nanoflow and microflow setups operating up to 5 μL/min, 50 μm ID capillaries for the 5–50 μL/min methods and 75 μm ID for the higher flow rates. We generally recommend using tubing lengths of 25–50 cm to achieve an optimal balance between minimizing dead volumes and ensuring ease of handling. As an example, our Waters M-Class LC setup typically operating at 2–5 μL/min comprises a 50 cm 25 μm Marvel XAct fittings for pump-to-autosampler and valve manager-to-column sections, and a 35 cm piece of the same dimensions for autosampler-to-valve manager connection. Column and M3 emitter are, in turn, linked via 25 or 35 cm 20 μm nanoViper capillary, as per manufacturer specifications. For the presented system, the pressure contribution from the fluidic connections typically ranges between 100 and 300 bars, depending on solvents and flow rates.

3.3 | Sample introduction

Lower flow rates necessitate the reduction of column dimensions. Consequently, smaller injection volumes are needed to strictly maintain chromatographic performance (Desmet & Eeltink, 2013; Vissers et al., 1997). For instance, a 300 μm ID column accommodates 0.04 μL of sample, equivalent to a 2 μL injection in an analytical setup (2.1 mm ID). However, such volume is already not available on most of the commercial instruments (typically min. 0.1 μL injection). In the context of nanoflow arrangements, equivalent injection volumes become even less practical. Although it is technically possible to provide on-column injections in single nanoliter volumes using specialized valves and/or custom-made injection loops, this technique is seldom used (Lubin et al., 2017; Vissers et al., 1996).

Employing relatively large injection volumes becomes possible as miniaturized bioanalytical applications pre-dominantly use gradient elution mode. When the analyte is injected in a solvent corresponding to a weaker composition than that needed for its isocratic elution, it's allowed to be focus as a thin band at the column head. Next, the elution occurs when gradient composition provides sufficient solvent strength (Ling et al., 1992). The injection volume for a microflow setup should not exceed 40% of the effective column volume (V_{col}) to avoid losses in chromatographic efficiency. However, minimal impact of the injection volume on strongly retained compounds on a C_{18}-based 0.3 mm ID column was observed when the injection band volume reached 160% of V_{col}. By contrast and as anticipated, a significant reduction in peak capacity occured primarily for weakly retained substances or those eluting in the void volume (Werres et al., 2021).

Commercial instruments commonly employ fixed split-loop injectors, which aspirate an exactly specified

aliquot of the sample bracketed by an injection solvent through a direct connection of a needle, sample loop and metering device (De Vos et al., 2016). These injectors can operate in either partial or full loop mode. The latter employs an overfill technique, ensuring maximal reproducibility, but at the cost of a higher sample consumption, typically 3–6 times the desired injection volume. In contrast, the partial loop mode sacrifices some accuracy and precision in favor of increased flexibility in method development. For microflow applications at 20–100 μL/min range, where an impact on gradient delay is less pronounced, flow-through-needle (FTN) injectors may be employed at a cost of increased band broadening effects (Broeckhoven et al., 2018; Deridder et al., 2018).

An alternative method of sample loading is related to the column switching approach. Here, a higher volume of the sample is introduced at higher flow rates (up to several hundred μL/min) onto a trapping column typically packed with large particles featuring high affinity for the analyte using a separate loading pump. Subsequently, matrix components, salts and impurities are either washed out with a loading solvent or selectively removed from the trap, if chromatographic separation on the trapping column is technically feasible. Next, analytes are transferred to the analytical column using a low-volume switching valve, either in front flush (analyte travels through the trap) or back flush (analyte eluted from the trap head) mode. To further increase the reliability of the system, a filter can be installed between the injector and the trap to capture particulate matter. The captured particulates are then flushed to waste in the backward direction using an additional pump and a system of switching valves. For microflow configurations, it is advisable to avoid transferring a single analyte plug from the trapping column with a strong solvent, as the volume of such a plug may be significant in comparison to the volume of the analytical column, potentially causing breakthrough. In addition, the retentivity of the trapping stationary phase should be lower compared to that of the analytical column to prevent excessive band broadening (Coppieters et al., 2021; Rochat et al., 2021; Rogeberg et al., 2014). The trap-and-elute configuration thus enables to make large volume injections (in the range of 10–20 μL on 0.3- and 0.15-mm ID columns) while minimizing problems related to particulates and loading capacity. It however requires the purchase of additional switching valves and auxiliary pumps.

3.4 | Chromatographic columns

Chromatographic columns for low flow setups can be categorized into two main groups: packed columns, filled with a suitable chromatographic material, and open tubular columns. In the first group, which is the most prevalent type in contemporary LC devices, columns are typically made of stainless steel or supported fused silica hardware. These columns are equipped with frits and filled with particles carrying a dedicated chromatographic functionality (C18, phenyl, amino, etc.) (Perchepied et al., 2022). This design offers high back-pressure resistance (up to 1500 bars), substantial sample loading capacity and the flexibility of employing various modes of interaction to separate different analyte groups (Kuehnbaum & Britz-McKibbin, 2013). The second group, encompassing open tubular columns, holds significant promise in chromatography. These columns achieve separation either in the porous layer of the column wall or on the wall coating layer (Mejía-Carmona et al., 2020). They exhibit characteristics such as high permeability and extraordinary chromatographic efficiencies in the order of multiple 10^5 of plates per meter. Contrary to gas chromatography, where such columns are regularly employed, only a few applications of those currently exists for LC, being primarily driven by fundamental research. These columns typically operate at extremely low flow rates due to their very narrow ID

(1–5 μm) and specific sample loading conditions. Importantly, they require highly customized instrumentation for their effective use. Given the special nature of these columns, we will not cover this topic here, but instead encourage the readers to the relevant literature for further exploration (Lam et al., 2019; Mejía-Carmona et al., 2020).

Another design which shows promise for microscale applications are monolithic columns. Such columns are prepared in situ by means of polymerization of a mixture of a suitable monomer and a porogen solvent. Size and morphology of the pores depend on properties of both counterparts and polymerization kinetics, whereas selectivity is provided by the type of monomer and functionalization (Premstaller et al., 2001; Urban & Jandera, 2008). The result is typically a continuous sponge-like bed, featuring macro- (1–10 μm), meso-(5–20 nm), and micropores (<5 nm). Macropores facilitate eluent flow-through, whereas mesopores provide a surface with active adsorption sites to facilitate the separation process (Moravcová et al., 2003). Although these columns provide better efficiency for macromolecules due to their porosity structure, it is possible to obtain higher efficiencies also for LMWC. A special interest of these columns for miniaturization comes from the ease of preparation in capillary format, absence of frits and higher permeability. Combined together, these properties allow for a robust long column with exceptional kinetic performance (Ishizuka et al., 2000;

Minakuchi et al., 1996). Despite these advantages, monolithic columns, after having gained momentum in the early 2000s, have become less widespread due to their lack of batch-to-batch reproducibility and are mainly available today via in-house synthesis. The only remaining major commercial provider for capillary and µLC formats is GLSciences (Japan). Interested readers can refer to the following literature for an in-depth view on the subject (Svec, 2017; Svec & Lv, 2015; Unger et al., 2008).

Chip-based columns constitute another prominent family of separation devices for µLC and can be considered by extension as silica monoliths. These columns are produced from silica using a photo-lithographic process similarly to the production of microprocessors, to create a channel for subsequent packing (Thurmann et al., 2015; Yin & Killeen, 2007) or an array of ordered pillars. The pillars are then etched and modified with a suitable ligand to form a stationary phase (He & Regnier, 1998; Vankeerberghen et al., 2023). Such pillar array columns, initially developed by the group of Desmet (Detobel et al., 2010) has been commercialized under the brand of µPAC^{TM} by Thermo Scientific. The advantages of these columns are lower flow resistance, excellent reproducibility of retention times and high efficiencies. The first generation of µPAC^{TM} featured 5 µm pillars separated by a 2.5 µm distance, whereas these values are halved on the second generation (Vankeerberghen et al., 2023). Despite their merits, their widespread adoption in bioanalysis is constrained by their cost and limited choice of stationary phase chemistries and dimensions. Nevertheless, successful applications of µPAC^{TM} in proteomics and lipidomics have been reported, with anticipation of more applications in the future (Rozing, 2021).

In the present review, we focus on packed microcolumns, due to their well-established technology and consistent market availability. It is generally admitted that these columns prove ideal for long-term routine method development, owing to their user-friendly nature, robust technology, ample sample loading capacity, and reliable lot-to-lot reproducibility. While µLC columns may exhibit lower chromatographic efficiency than conventional columns, it is worth highlighting that the primary goal of low flow methods is signal amplification rather than outstanding chromatographic performance. Besides, compared to their analytical counterparts, capillary columns suffer less from frictional heating and wall effects, which might partially compensate for the lower chromatographic efficiency (Gritti & Wahab, 2018; Gritti et al., 2016). Although columns with smaller IDs are more limited in terms of particles chemistries, the µLC niche has not been completely overlooked by the market, and there is a good offer of relevant column formats bonded with various ligands. Table 3 summarizes relevant products offered by major vendors in a timely and reproducible fashion. The emphasis is on modern, highly efficient packings with fully (FPP) or superficially (SPP) porous particles, featuring standard connections designed to withstand higher backpressures (Figure 3). Besides, the advantage of lower flow resistance of superficially porous particles can be easily exploited in µLC setups, as higher linear velocities are conveniently accessible with µLC pumps. This approach proves particularly fruitful for high throughput methods, minimizing losses in resolution while enabling shorter analysis time (González-Ruiz et al., 2015; Tanaka & McCalley, 2016). As an illustration, the transfer from a 2.1×150 mm column ($2.7 \, \mu m$) at 1 mL/min to a 0.5×150 mm column would allow for approximately 60 µL/min flow rates at 850 bars while maintaining most of the method resolution and greatly increasing detection limits.

The majority of the presented columns prominently feature various types of C_{18} ligands, primarily tailored for RP separations. This choice aligns with the versatility of the RP approach and its historical application in the separation of tryptic digests in bottom-up proteomics (Lenčo et al., 2022). Nevertheless, alternative separation modes such as hydrophilic interaction liquid chromatography (HILIC) are also available in miniaturized formats. Several vendors, particularly Merck (ZIC), AMT and YMC (Diol), offer columns tailored for HILIC applications. The utility of HILIC phases is somewhat limited due to the absence of readily available hardware with reduced nonspecific adsorption. Hence the analysis of polar compounds with increased sensitivity requirements, such as certain pesticides, phosphorylated peptides/lipids and oligonucleotides, is hindered by their capacity to bind to metal surfaces (Guimaraes & Bartlett, 2023). A monolithic capillary column with embedded amide functionality in PEEK hardware (GL Sciences; MonoCap Amide) may represent an interesting commercial option in this particular case.

Modern µLC columns exhibit robustness enabling them to withstand frequent pressure fluctuations of varying frequency and amplitude, as outlined in their specifications. However, it is strongly recommended to avoid rapid pressure drops and unnecessary decompression, considering the overall higher fragility of miniaturized instrumentation. The absolute loading capacity of microcolumns is significantly lower compared to conventional ones, making matrix build-up effects more pronounced. To ensure a reliable method able to handle large batches, a practical rule of thumb is "to elute everything towards the end of the gradient."

TABLE 3 An overview of well-established columns with high kinetic performance (sub 2 μm or sub 3 core shell) for microscale LC/ESI-MS analysis (major vendors, as of 01.11.2023).

Vendor	Waters	ChromaNik	AMT	Phenomenex	YMC	Thermo Scientific	Bruker
Brand(s)	nanoEase MZ Acquity UPLC	SunShell	Halo	Kinetex Luna Omega	-	Hypersil Gold uPac Neo	PepSep
Length, mm	50, 100, 150	50, 150	50, 100, 150	50, 100, 150	50, 100, 150	55, 50, 100	50, 80, 100, 150, 250
Hardware	Stainless steel	Steel, PEEK/fused silica	Steel, PEEK/fused silica	Stainless steel	Steel/fused silica	Steel, Silicon (μPAC)	PEEKSil
Column ID, μm	Available column chemistry						
150	-	-	-	-	-	μPAC C_{18}	C_{18}, C_{18}-Aq
200	-	C_{18}, Phenyl	-	-	-	-	-
300	BEH, CSH, HSS T3[a]		All major chemistries[b]	All major chemistries	All Triart phases		
500	-						
1000	All major chemistries	2.0 SPP	2.7 SPP	Biphenyl, C_{18}, Polar C_{18}	C_{18}	C_{18}, C_{18}-Aq, C_8	
Particle size, μm	1.7, 1.8 FPP	2.0 SPP	2.7 SPP	1.6 FPP, 2.6 SPP	1.9 um FPP	2.5 pillar, 1.9 FPP	1.5, 1.9 FPP
Backpressure, bar	1000	800	600	1000	600	1000	1000
Temperature, °C	80	80	50	50	80	50	60
Guard	filter 0.2 μm, steel	n/a	n/a	Filter 2 μm, steel	Yes	Yes	n/a
Trap	For 300 μm C_{18}	n/a	n/a	For C_{18} phases	Guard	Yes	Yes

[a]All phases feature C18 ligand: BEH, bridged ethylene hybrid; CSH, charged surface hybrid; HSS T3, high-strength silica with low-density triple-bound ligand.
[b]Recently introduced stationary phases may be unavailable.

Given the constraints of miniaturized systems, rapid switching between mobile phases is unfeasible. Therefore, it is advised to employ stronger eluents in combination with more gentle gradient slopes to provide column wash of sufficient strength.

3.5 | Ionization sources and mass spectrometry considerations

The ionization source plays a pivotal role in any microflow setup, defining the efficiency of ESI and, consequently, the sensitivity improvement. Furthermore, the spray characteristics can be significantly influenced by the material and geometry of the emitter (Maxwell et al., 2010; Reschke & Timperman, 2011). The fundamental concept behind the design of any microflow ionization source is to minimize the extra-column volume and the dimensionality of the sprayer. In the majority of cases, sensitivity improvements compared to the classical approach may be achieved using flow rates between 50 and 100 µL/min on core-shell 0.5 mm or fully porous 1.0 mm ID columns. In this case, the MS vendor's microspray option is the most practical and economical choice (Figure 3). Typically, such options are provided by the MS instrument vendor as a separate device (e.g., Shimadzu, Sciex) or as the possibility to replace the conventional ESI needle with one of a smaller ID (usually 50 µm needle) in the case of Bruker (Midha et al., 2023), Thermo Scientific and Waters. For lower flow rates, a customization of the ionization source is required by forging the needle insert with the reduced ID, for example, EASY-Spray Jailbreak (Phoenix S&T; Thermo), microflow ion source (Prolab GmbH, Switzerland; Sciex) and DuoESI (Newomics; Thermo, Bruker, Agilent, Shimadzu). The latter is of a particular interest, featuring a unique microfabricated monolithic multi-nozzle (M3) sprayer, that divides the incoming flow into multiple streams, transitioning from microflow LC to nanospray (Kim et al., 2007; Mao et al., 2011). This design has a potential to maximize sensitivity by combining higher mass loads with the most efficient ionization. An alternative involves an integrated approach, combining fluidic connections, a heater, a column and a sprayer into a single module (Broccardo et al., 2013). Represented by devices such as ionKey (300 and 150 µm ID; Waters) and EASY-Spray (150 µm ID; Thermo), this family offers a key advantage with practically nonexistent extra-column volume. The embedded column is directly connected to a sprayer, resembling nano-LC setups, and produces sharply defined chromatographic peaks. Samples are typically loaded onto such integrated devices via trapping,

providing additional protection for this otherwise expensive part.

In all scenarios, some degree of manual optimization is inevitable. The primary objective is to achieve a stable spray as close as possible to the sprayer inlet, ensuring maximum sampling of the stable ESI plume into the spectrometer (Bonvin et al., 2012). Simultaneously, efforts are directed towards minimizing adverse effects such as analyte deposition resulting from sprayer overheating, electric discharges, and fouling (or even blockage) of the ion transfer region with residues of complex matrices, as demonstrated by Rochat et al. (2021). These detrimental effects have to be reduced to the absolute minimum to guarantee a reproducible analysis of large batches.

Finally, the increased ion currents resulting from the combination of µLC with the optimized ionization source will lead to increased wear of ion optics and detectors within the mass spectrometer. Logically, a more frequent cleaning of ion optics may be necessary. In contrast with triple quadrupole (QqQ) and orbitrap mass spectrometers which feature spatial separation and management of the incoming ion current by design, multichannel plate detectors of time-of-flight (TOF) instruments may be prone to a quick saturation (Liu et al., 2014; Westman et al., 1997) and rapid detector wear if ion current control measures are not enabled or implemented (Ibrahim et al., 2008; Syka et al., 2004). On the other hand, TOF instruments feature better analytical coverage compared to trap-based mass analyzers due to the absence of space charge capacity limitations.

4 | SETTING UP A ROBUST MLC/ESI-MS WORKFLOW

4.1 | Methodological considerations

As mentioned in Ch. 3.4, the major driver for employing miniaturized LC/ESI-MS coupling stems from the necessity to reliably detect low-abundant analytes within a relatively large sample matrix. Therefore, the evaluation of the applicability of µLC/ESI-MS, beyond equipment availability, hinges on the convergence of the chemical properties of the matrix/analyte combination and the desired detection levels of the method. When dealing with very low-abundant analytes, a systematic approach should be adopted in designing a prospective microflow setup. To assist in this decision-making process, we provide a scheme that succinctly outlines methodological considerations for microflow setups, considering the desired sensitivity levels and compatible sample preparation techniques to handle matrix

complexity. Our ultimate aim is to achieve the highest possible sensitivity while maintaining chromatographic performance. Therefore, it is essential to account for the total mass load when analyzing biological matrix. Matrix interferences will inevitably compete for the available stationary phase adsorption sites thus reducing the loading of the target analyte compared to injections in a neat solution. Consequently, biological samples may require appropriate dilution or adjustment of the preconcentration factor during sample preparation (Figure 4).

Importantly, the targeted or nontargeted nature of the application should be considered. Targeted and semi-targeted analysis typically focus on a limited number of analytes, involving specific sample preparation procedure with extensive cleanup. Conversely, nontargeted studies aim to encompass a broad sample chemical space, leading to increased contaminants and matrix compounds due to simplified sample preparation methods, such as protein precipitation (plasma) or simple dilution (urine). For nontargeted analyses requiring minimal sample preparation in complex matrixes, it is preferable to use 20–80 μL/min flow rates with columns of 0.5- or 1.0-mm ID. This analytical approach is particularly effective when paired with stainless-steel emitters of relatively large ID (50–75 μm). This combination minimizes the impact of matrix components during

continuous analysis of large batches, thus increasing system robustness. Although it is possible to inject samples prepared in the nontargeted fashion onto columns of smaller ID at lower flow rates to further increase the analytical signal, special precautions should be taken during sample preparation (e.g., suitable solvent composition to avoid precipitation, avoiding overload, compulsory filtration before injection, etc.).

We cannot emphasize enough that maximal sample cleanup should be a continual objective in low and capillary μLC/ESI-MS measurements. First, it is imperative to eliminate non-volatile compounds such as salts, as they can undesirably accumulate on the emitter tip. Second, considering the limited loading capacity of microcolumns, the ideal sample should exclusively consist of the analyte to fully occupy the available particle surface. For complex biological matrices, such as plasma, serum or seminal fluid, desalting, deproteiniza-tion and delipidation are crucial. This can be achieved through salt-assisted liquid–liquid extraction (SALLE)(Liu et al., 2019), or a carefully designed elution from SPE cartridge (David et al., 2014; Seidi et al., 2019). To eliminate protein residues, a protein crush step before SPE is essential (Thomas et al., 2013). We recommend to allow for overnight precipitation at a temperature of at least −20°C and repeat the centrifugation step twice before injection. Alternatively, LLE is a fast and easy to
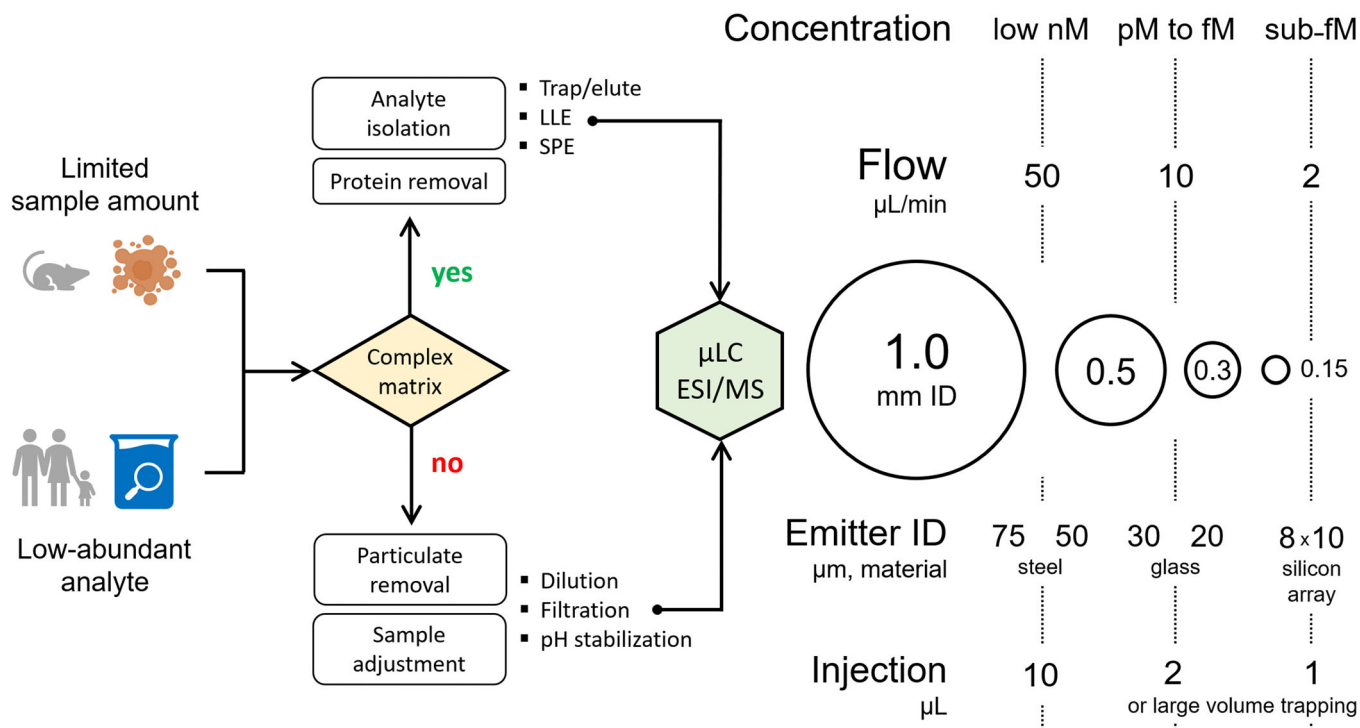
FIGURE 4 An approach to a rational selection of miniaturized liquid chromatography/electrospray ionization mass spectrometry setup based on targeted analyte concentration. [Color figure can be viewed at wileyonlinelibrary.com]

handle method that typically eliminates salt, protein or lipid transfer into the sample (Shen et al., 2013; Souverain et al., 2004; Zardini Buzzato et al., 2020), although it is less suitable for polar compounds. Miniaturization works well for LLE, allowing for a highly favourable solvent-to-sample ratio. For an optimal cleanup, mixed-mode SPE may provide the best solution due to the variety of interactions involved (Gilar et al., 2008; Nadal et al., 2022).

Following the reconstitution step, it is recommended to filter the sample using a spin filter or a well plate of at least 0.2 µm to prevent particulates in the narrow channels of the injector and autosampler. Molecular weight cutoff filters present an even better alternative, enabling selective deproteinization. However, filtration times may be prolonged, especially for 3K-cutoff filters and/or in presence of high viscosity solvents or when filtering at lower temperatures. Finally, an attention should be given to potential nonspecific adsorption of analytes to the filter material and other surfaces.

4.2 | Advantages and pitfalls of µLC/ESI-MS: Theory becomes practice

Based on our experience, a substantial 4–10× improvement in peak area can be consistently achieved with minimal challenges when transitioning from standard ionization sources to reduced ESI needles adapted to flow rates <100 µL/min (column ID 0.5–1.0 mm). Such benefit is illustrated in Figure 5A, where we analyzed the Pierce peptide mix using columns of identical length (150 mm) and chemistry, but differing in diameter to assess the performance of µLC/ESI-MS. The improvement in sensitivity is evident, albeit with a slight trade-off in chromatographic performance. For instance, the baseline width of the Pierce 5 peptide peak was 0.10 min on a 2.1 ID column, while it increased to 0.14 min for the 1.0- and 0.5-mm ID counterparts. Interestingly, for the Pierce 6 peptide, while the first reduction of ID (2.1 > 1.0 mm) only provides a 1.7-fold increase in peak intensity, the second reduction (1.0 > 0.5 mm ID) provides an over threefold increase. This can be unequivocally attributed to the use of a more suitable ESI emitter for the given flow rate (50 vs. 100 µm needle). Different physico-chemical properties of both compounds may also contribute to intrinsic ionization efficiency, which explains uneven signal gains. In addition, the enhanced availability of charges may induce shifts between charge states in the microflow regime, particularly for analytes like peptides or natural products with multiple ionisation sites. Quantitative work should consider the charge state distribution, as well as the possible presence of newly formed adducts and their ratios. Similarly to small peptides, an eightfold improvement in peak area was obtained for LMWC in matrix conditions, as illustrated with cortisol in the course of nontargeted profiling of human plasma samples (Figure 5B).

From a practical standpoint, we realized that the ion source design plays a crucial role in the absolute improvement of the analytical signal and that precise optimization of ion sampling with original ion sources was challenging. *Y*-axis adjustment was absent on the Waters instrument and HESI II on a Thermo QExactive machine faced arcing issues. Additionally, neither of the sources featured a camera and internal lamp to visualize the spray plume during analysis, hindering reasonable voltage/gas flow adjustments and emitter tip observation during analysis. Based on this experience, we took a significant step forward by employing a 0.3 mm ID column at a flow rate of 6 µL/min, with a novel M3 emitter on Orbitrap Exploris 120. This approach allowed us to simultaneously achieve increased ion yields, observe the spray and reduce nonspecific adsorption in the system due to the more inert material of the nozzles. Analyzing a depleted plasma sample prepared through multiple filtration and SPE after careful optimization revealed a remarkable improvement of more than two orders of magnitude for cortisol. However, an approx. 6x reduction in chromatographic peak capacity was observed due to the massive volumetric overload (1 µL on a 0.3 mm ID column corresponds to 50 µL on a 2.1 mm ID column) (Figure 5C). This last example shows all the potential of µLC/ESI-MS compared to standard analytical conditions.

5 | CURRENT BIOANALYTICAL APPLICATIONS AND METHODS FOR LMWC

In this section we present a compilation of studies spanning from 2018 to 2023 that have employed micro-flow approaches coupled to mass spectrometry for bioanalytical applications (Table 4). Despite the relatively small number of microflow applications focused on LMWC, several emerging trends can already be identified.

First of all, it is obvious that these bioanalytical applications primarily target specific families of compounds and often utilize sample and injection volumes similar to those in established analytical setups. For instance, Aydin et al. achieved the analysis of cortisone and cortisol from saliva by subjecting 700 µL of this biofluid to an SPE on Oasis PRIME 96-well plate, a widely used material in steroid analysis. Here, a
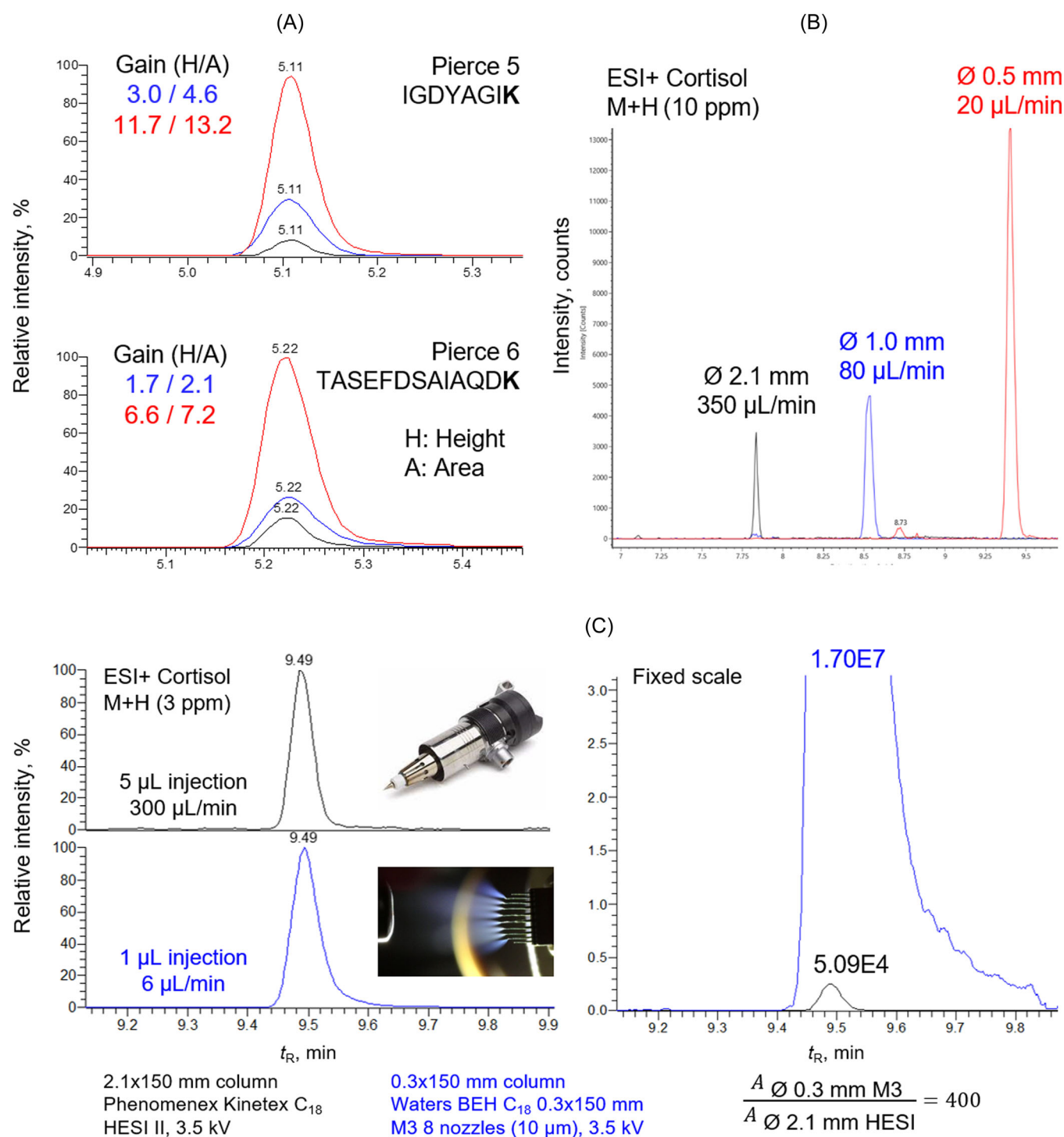
FIGURE 5 Selected ion chromatograms (SIC) of (A) Pierce® peptides, (B) endogenous steroid cortisol on 150 mm YMC Triart C_{18} columns with the corresponding reduction of flow rates, and (C) on a 0.3 mm ID column with novel M3 emitter versus analytical column with conventional HESI II source. [Color figure can be viewed at wileyonlinelibrary.com]

relatively large injection volume of 5 μL was made onto a 0.5 mm ID column. Such volume would correspond to a 88 μL injection on a classical 2.1 mm ID column of the same dimensions, resulting in approx. 17.5× overload factor (Aydin et al., 2021). Kafeenah et al. detected estrogens and their metabolites at a level of as low as

60 pM from 200 μL of serum using a 3 μL injection onto a 220 × 0.2 mm column (overload factor 110) via trapping (Kafeenah et al., 2022). Finally, He et al. worked at the overload factor of 50, injecting 3 μL of sample onto a 0.3 mm ID column (He et al., 2022). This tendency to use large overload factors likely arises from the widespread

TABLE 4 Selected studies from 2018 to 2023 applying μLC/ESI-MS approach in capillary to semi-microflow regimes.

Workflow	Matrix	$V_{biofluid}$, μL	V_{sample}, μL	LC model	Column	Flow, μL/min	Detection limits, pM	MS model	Ref.
Targeted quantitative analysis									
Endocannabinoids	Cerebrospinal fluid	250	3	Waters nanoAcquity	Phenomenex C_{18} 150 × 0.3 mm (2.6 μm)	4	0.7–1293	Shimadzu 8060 (micro-ESI) MRM, 30 μm ID TaperTip	He et al. (2022)
Peptide hormones	Human plasma	50	7 on trap	Waters M-Class	Waters ionKey Peptide BEH 150 × 0.15 mm (1.7 μm)	3	4–200	Waters G2-XS Q-TOF, full scan Waters TQ-XS, MRM	Chen et al. (2019)
Cortisol, cortisone	Saliva	700	5	Sciex Eksigent MicroLC 200	YMC Triart C_{18} 50 × 0.5 mm (3 μm)	20	28–56	Sciex QTRAP 4500 MRM, 50 μm electrode	Aydin et al. (2021)
Drugs & metabolites	Primate plasma	25	2	Sciex M5 MicroLC	AMT Halo C_{18} 50 × 0.2 mm (2.7 μm)	5.4	150–300	Sciex API6500 MRM, OptiFlow source	Barricklow et al. (2020)
Estrogen metabolites	Human serum	200	3 on trap	Waters nanoAcquity	Home-packed BEH C_{18} 220 × 0.2 mm (1.7 μm)	1.7	60–1439	Sciex QTRAP 4000 MRM, 20 μm emitter	Kafeenah et al. (2022)
Drugs & metabolites	Neonatal plasma	25	0.5	Sciex Eksigent 2D Plus	Waters 100 × 0.15 mm (1.7 μm)	1	35–175	Sciex TripleTOF 5600+SWATH, PicoView 450 source	Xiao et al. (2021)
Peptide hormones	Diluted plasma	900	250 on trap	Thermo Scientific Ultimate 3000 RSLCnano	Diverse RP-type 50–150 mm, 0.2–0.3 mm ID	10	2.5–250	Thermo QExactive Plus Full scan + DDA, M3 source	Rochat et al. (2021)
Nontargeted and structural applications							Improvements		
Profiling of urea cycle disorder mouse model	Mouse urine, brain	20 urine 20 brain	0.8	Waters M-Class	Waters HSS SB C_{18} Imtakt Scherzo SM-C_{18}	86	Not specified	Thermo QExactive Full scan, 50 μm electrode	Geller et al. (2022)
Investigation of miniaturization impact on wide-scale analysis	Human plasma	100	3	Thermo Scientific Vanquish Duo	Waters HSS T3 C_{18} 150 × 1.0 mm (1.7 μm)	57	Not specified	Thermo QExactive HF Full scan, 50 μm electrode	Fitz et al. (2022)

(Continues)

TABLE 4 (Continued)

Workflow	Matrix	$V_{biofluid}$, µL	V_{sample} µL	LC model	Column	Flow, µL/min	Detection limits, pM	MS model	Ref.
Identification of drug metabolites	Mouse plasma	75	5	Waters M-Class	Waters ionKey BEH C$_{18}$ 50×0.15 mm (1.7 µm)	3	Not specified	Waters G2-XS Q-TOF	Majewsky et al. (2018)
Investigation of HILIC in µLC conditions	Porcine kidney	tissue	1	Prolab Zirconium Ultra	Custom BEH amide HILIC 150×0.3 mm (1.7 µm)	5	80× more signal for bile acids	Agilent 6550 iFunnel QTOF Prolab micro-ESI interface	Neef et al. (2023)
Technological advancements									
Coupling with differential ion mobility	Glycopeptides	2 µM solution	2	Shimadzu Nexera Mikros	AMT Halo C$_{18}$ 100×0.5 mm (1.7 µm)	20	Not specified	Sciex TripleTOF 6600 + Micro probe, DMS cell	Jacquet and Hopfgartner (2022)
Coupling with vibrating sharp-edge spray ionization	Tryptic digest Metabolites Nucleotides	Diverse	n/a	Flow splitting	Analytical LC to 0.36 mm ID fused silica capillary	30	Better ionization efficiency	Thermo QExactive Full scan, custom ion source	Majuta et al. (2021)
Coupling with atmospheric pressure chemical ionization	Acridine	50 µM solution	0.1	Sciex ExionLC AD	Agilent Zorbax XDB-C$_{18}$ 150×0.5 mm (3.5 µm)	10	10× more ion yield	Thermo LCQ Fleet ion trap Full scan, custom ion source	Strmeň et al. (2018)
Implementation of µ-(2D-LC) separation	Human plasma	200	0.5	Waters I-class 2D configuration	100×1.0 mm BEH amide (1D) 150×1.0 mm HSS T3 C$_{18}$ (2D)	100	Higher annotation rates	Waters Synapt G2-Si Thermo LTQ Orbitrap XL	Orlandi et al. (2023)

need to achieve the highest concentration of minute quantities of challenging compounds from larger volumes of biological matrix. In addition, these results demonstrate a sufficient loading capacity of both SPP- and FPP-based stationary phases, given the effort undertaken at the sample preparation step to eliminate matrix components.

Another remarkable trend observed across the existing literature is the use of customized ionization sources to achieve μLC/ESI-MS analysis. Only 30% of the works feature 50 μm ID electrospray needles, the most common and accessible solution to work with lower flow rates. The remaining setups rely on a customized high-performance solution, either commercially acquired or developed in-house (Barricklow et al., 2020; Chen et al., 2019; He et al., 2022; Jacquet & Hopfgartner, 2022; Kafeenah et al., 2022; Majewsky et al., 2018; Majuta et al., 2021; Neef et al., 2023; Rochat et al., 2021; Strmeň et al., 2018; Xiao et al., 2021). These findings are further supported by our practical experience demonstrated in Ch. 4 and strongly reinforce the ionization source design as the most crucial contributor to the wider implementation of μLC/ESI-MS approaches.

Since sensitivity improvement could be considered as the primary driver behind employing miniaturization, a wider occurrence of QqQ systems was expected, especially given their dominance in quantitative studies related to LMWC. However, only 6 of 15 works in this review were performed on such instruments, whereas the majority relied on high-resolution mass spectrometers (HRMS). This low amount of μLC-QqQ applications may highlight an additional benefit of having HRMS data for re-exploration while being able to monitor elusive analytes once only detectable with more sensitive QqQ instruments. Notably, HRMS instruments coupled to μLC provided lower limits of quantitation due to enhanced selectivity (Chen et al., 2019) and demonstrated that quantitation can be achieved with different scan modes, such as full scan (Rochat et al., 2021), sequential window acquisition of all theoretical spectra (SWATH) (Xiao et al., 2021), and alternating all-ion fragmentation (Chen et al., 2019). Overall, four of the discussed studies (Aydin et al., 2021; He et al., 2022; Kafeenah et al., 2022; Rochat et al., 2021) featured validated protocols, whereas two were performed with >100 samples in a batch (Aydin et al., 2021; He et al., 2022).

Nevertheless, the capability to handle low sample volumes as a distinguishing feature of the miniaturized analytical setups still remains unquestionable, as demonstrated by Barricklow et al. (2020) Chen et al. (2019). Geller et al. exploited this advantage to conduct an exploratory analysis of mouse brain homogenates investigating urea cycle disorder (Geller et al., 2022). Notably, their works also illustrated the feasibility of measuring polar compounds in negative ESI mode using μLC (Geller et al., 2021), although the spray in negative mode tends to be less stable in nano-LC-based setups (McClory & Håkansson, 2017). Microflow HILIC can be a potent alternative to the mixed-mode chromatography for polar compounds. Neef et al. used an in-house packed BEH amide column, demonstrating an 80-fold improvement in bile acid analysis compared to conventional systems. However, they also noted nonuniform response to miniaturisation, with S/N ratio being better in only 50% of the analytes (Neef et al., 2023). Finally, the capability of μLC/ESI-MS to produce high ion current for better fragmentation data was employed in structural studies of the anthelmintic benzimidazole and its metabolites in mice (Majewsky et al., 2018).

Overall, the μLC approach offers an optimal compromise between sensitivity improvement and metabolome coverage in nontargeted studies, as demonstrated by Fitz et al. (2022). Not surprisingly, a rather moderate increase in overall method performance was obtained at the higher range of the microflow region (57 μL/min, 1 mm ID column). However, this increase came practically at no cost, as the microbore column employed and corresponding flow rates are supported by classical binary LC systems. Reducing the flow rate and, consequently, facilitating the management of smaller effluent volumes, is also a potent driver for the advancements of LC and MS technologies. Both emerging (Majuta et al., 2021) and established ionization methods, including atmospheric pressure chemical ionization (Strmeň et al., 2018), exhibit improved performance when operating under microflow conditions. Introducing additional separation dimensions, such as orthogonal two-dimensional chromatography (Orlandi et al., 2023) or differential ion mobility (DIM)(Jacquet & Hopfgartner, 2022) are accessible to further improve the selectivity of miniaturized setups. Moreover, coupling of μLC with DIM has revealed the influence of eluent on DIM separation in the analytical flow regimes (Girard et al., 2022).

6 | CONCLUDING REMARKS

The limited utilisation of μLC approaches in bioanalysis within the existing literature is somehow disheartening, especially considering that advantages of miniaturized systems date back from the 1970s. Recent advancements have propelled analytical instruments towards increased robustness, accuracy and precision, complemented by the availability of precision-crafted consumables for

microanalysis. As practically demonstrated by specific examples, reliable measurements using hyphenated miniaturized chromatography have now become accessible to a wider audience. The increased sensitivity of analytical platforms resulting from these advancements holds the potential to dramatically improve the quantitative results of both targeted and semi-targeted methods. Moreover, higher ion currents generated by miniaturized systems prove advantageous for emerging alternative fragmentation methods, particularly those suffering from low precursor conversion, such as electron-activated dissociation (Baba et al., 2021). This opens up new possibilities to uncover a wealth of structural information about metabolites, environmental compounds, and xenobiotics that reside in the lower end of an organism's concentration range. Consequently, this expansion in our analytical capabilities has the potential to deepen our understanding of both biological and environmental processes.

AUTHOR CONTRIBUTIONS

Sergey Girel: Conceptualization; data curation; formal analysis; investigation; writing—original draft. **Isabel Meister**: Conceptualization; investigation; writing—original draft. **Gaetan Glauser**: Conceptualization; resources; writing—review and editing. **Serge Rudaz**: Conceptualization; resources; supervision; writing—review and editing.

CONFLICT OF INTEREST STATEMENT

The authors declare no conflict of interest.

ORCID

Sergey Girel http://orcid.org/0000-0002-8165-537X

REFERENCES

J. Abian, A. J. Oosterkamp, E. Gelpi, Comparison of conventional, narrow-bore and capillary liquid chromatography/mass spectrometry for electrospray ionization mass spectrometry: practical considerations, *J. Mass Spectrom. 34* (1999) 244–254.

A.-F. Aubry, LC–MS/MS bioanalytical challenge: ultra-high sensitivity assays, *Bioanalysis 3* (2011) 1819–1825. https://doi.org/10.4155/bio.11.166

E. Aydin, B. Drotleff, H. Noack, B. Derntl, M. Lämmerhofer, Fast accurate quantification of salivary cortisol and cortisone in a large-scale clinical stress study by micro-UHPLC-ESI-MS/MS using a surrogate calibrant approach, *J. Chromatogr. B 1182* (2021) 122939. https://doi.org/10.1016/j.jchromb.2021.122939.

T. Baba, P. Ryumin, E. Duchoslav, K. Chen, A. Chelur, B. Loyd, I. Chernushevich, Dissociation of biomolecules by an intense low-energy electron beam in a high sensitivity time-of-flight mass spectrometer, *J. Am. Soc. Mass Spectrom. 32* (2021) 1964–1975. https://doi.org/10.1021/jasms.0c00425

U. Bahr, A. Pfenninger, M. Karas, B. Stahl, High-sensitivity analysis of neutral underivatized oligosaccharides by nanoelectrospray mass spectrometry, *Anal. Chem. 69* (1997) 4530–4535. https://doi.org/10.1021/ac970624w

S. Banerjee, Empowering clinical diagnostics with mass spectrometry, *ACS Omega 5* (2020) 2041–2048. https://doi.org/10.1021/acsomega.9b03764

J. Barricklow, J. Tweed, C.L. Holliman, R. Ramanathan, Evaluation of OptiFlow™-MS/MS for bioanalysis of pharmaceutical drugs and metabolites, *Bioanalysis 12* (2020) 23–34. https://doi.org/10.4155/bio-2019-0250

M.S. Bello, R. Rezzonico, P.G. Righetti, Use of Taylor-Aris dispersion for measurement of a solute diffusion coefficient in thin capillaries, *Science 266* (1994) 773–776. https://doi.org/10.1126/science.266.5186.773

Y. Bian, C. Gao, B. Kuster, On the potential of micro-flow LC-MS/MS in proteomics, *Expert Rev. Proteomics 19* (2022) 153–164. https://doi.org/10.1080/14789450.2022.2134780

Y. Bian, R. Zheng, F.P. Bayer, C. Wong, Y.-C. Chang, C. Meng, D.P. Zolg, M. Reinecke, J. Zecha, S. Wiechmann, S. Heinzlmeir, J. Scherr, B. Hemmer, M. Baynham, A.-C. Gingras, O. Boychenko, B. Kuster, Robust, reproducible and quantitative analysis of thousands of proteomes by micro-flow LC–MS/MS, *Nat. Commun. 11* (2020) 157. https://doi.org/10.1038/s41467-019-13973-x

G. Bonvin, J. Schappler, S. Rudaz, Capillary electrophoresis–electrospray ionization-mass spectrometry interfaces: fundamental concepts and technical developments, *J. Chromatogr. A 1267* (2012) 17–31. https://doi.org/10.1016/j.chroma.2012.07.019

C.J. Broccardo, K.L. Schauer, W.M. Kohrt, R.S. Schwartz, J.P. Murphy, J.E. Prenni, Multiplexed analysis of steroid hormones in human serum using novel microflow tile technology and LC–MS/MS, *J. Chromatogr. B 934* (2013) 16–21. https://doi.org/10.1016/j.jchromb.2013.06.031

K. Broeckhoven, K. Vanderlinden, D. Guillarme, G. Desmet, On-tubing fluorescence measurements of the band broadening of contemporary injectors in ultra-high performance liquid chromatography, *J. Chromatogr. A 1535* (2018) 44–54. https://doi.org/10.1016/j.chroma.2017.12.032

N.B. Cech, C.G. Enke, Relating electrospray ionization response to nonpolar character of small peptides, *Anal. Chem. 72* (2000) 2717–2723. https://doi.org/10.1021/ac9914869

N.B. Cech, C.G. Enke, Practical implications of some recent studies in electrospray ionization fundamentals, *Mass Spectrom. Rev. 20* (2001) 362–387. https://doi.org/10.1002/mas.10008

Z. Chen, Y.W. Alelyunas, M.D. Wrona, J.R. Kehler, M.E. Szapacs, C.A. Evans, Microflow UPLC and high-resolution MS as a sensitive and robust platform for quantitation of intact peptide hormones, *Bioanalysis 11* (2019) 1275–1289. https://doi.org/10.4155/bio-2019-0081

A.J. Chetwynd, A. David, A review of nanoscale LC-ESI for metabolomics and its potential to enhance the metabolome

coverage, *Talanta 182* (2018) 380–390. https://doi.org/10.1016/j.talanta.2018.01.084

N.J. Clarke, Mass spectrometry in precision medicine: phenotypic measurements alongside pharmacogenomics, *Clin. Chem. 62* (2016) 70–76. https://doi.org/10.1373/clinchem.2015.239475

G. Coppieters, K. Deventer, P. Van Eenoo, P. Judák, Combining direct urinary injection with automated filtration and nano-flow LC-MS for the confirmatory analysis of doping-relevant small peptide hormones, *J. Chromatogr. B 1179* (2021) 122842. https://doi.org/10.1016/j.jchromb.2021.122842

N. Danne-Rasche, C. Coman, R. Ahrends, Nano-LC/NSI MS refines lipidomics by enhancing lipid coverage, measurement sensi-tivity, and linear dynamic range, *Anal. Chem. 90* (2018) 8093–8101. https://doi.org/10.1021/acs.analchem.8b01275

A. David, A. Abdul-Sada, A. Lange, C.R. Tyler, E.M. Hill, A new approach for plasma (xeno)metabolomics based on solid-phase extraction and nanoflow liquid chromatography-nanoelectrospray ionisation mass spectrometry, *J. Chromatogr. A 1365* (2014) 72–85. https://doi.org/10.1016/j.chroma.2014.09.001

J. De Vos, K. Broeckhoven, S. Eeltink, Advances in ultrahigh-pressure liquid chromatography technology and system design, *Anal. Chem. 88* (2016) 262–278. https://doi.org/10.1021/acs.analchem.5b04381

S. Deridder, G. Desmet, K. Broeckhoven, Numerical investigation of band spreading generated by flow-through needle and fixed loop sample injectors, *J. Chromatogr. A 1552* (2018) 29–42. https://doi.org/10.1016/j.chroma.2018.04.001

G. Desmet, S. Eeltink, Fundamentals for LC miniaturization, *Anal. Chem. 85* (2013) 543–556. https://doi.org/10.1021/ac303317c

F. Detobel, S. De Bruyne, J. Vangelooven, W. De Malsche, T. Aerts, H. Terryn, H. Gardeniers, S. Eeltink, G. Desmet, Fabrication and chromatographic performance of porous-shell pillar-array columns, *Anal. Chem. 82* (2010) 7208–7217. https://doi.org/10.1021/ac100971a

C.G. Enke, A predictive model for matrix and analyte effects in electrospray ionization of singly-charged ionic analytes, *Anal. Chem. 69* (1997) 4885–4893. https://doi.org/10.1021/ac970095w

P.W. Fedick, R.M. Bain, S. Miao, V. Pirro, R.G. Cooks, State-of-the-art mass spectrometry for point-of-care and other applications: A hands-on intensive short course for undergraduate students, *Int. J. Mass Spectrom. 417* (2017) 22–28. https://doi.org/10.1016/j.ijms.2017.04.008

V. Fitz, Y. El Abiead, D. Berger, G. Koellensperger, Systematic investigation of LC miniaturization to increase sensitivity in wide-target LC-MS-based trace bioanalysis of small molecules, *Front. Mol. Biosci. 9* (2022) 857505. https://doi.org/10.3389/fmolb.2022.857505

S. Geller, H. Lieberman, A. Kloss, A.R. Ivanov, A systematic approach to development of analytical scale and microflow-based liquid chromatography coupled to mass spectrometry metabolomics methods to support drug discovery and development, *J. Chromatogr. A* 2021 (*1642*) 462047. https://doi.org/10.1016/j.chroma.2021.462047

S. Geller, H. Lieberman, A.J. Belanger, N.S. Yew, A. Kloss, A.R. Ivanov, Comparison of microflow and analytical flow liquid chromatography coupled to mass spectrometry global metabolomics methods using a urea cycle disorder Mouse Model, *J. Proteome Res. 21* (2022) 151–163. https://doi.org/10.1021/acs.jproteome.1c00628.

H.G. Gika, G.A. Theodoridis, R.S. Plumb, I.D. Wilson, Current practice of liquid chromatography–mass spectrometry in metabolomics and metabonomics, *J. Pharm. Biomed. Anal. 87* (2014) 12–25. https://doi.org/10.1016/j.jpba.2013.06.032

M. Gilar, Y.-Q. Yu, J. Ahn, J. Fournier, J.C. Gebler, Mixed-mode chromatography for fractionation of peptides, phosphopep-tides, and sialylated glycopeptides, *J. Chromatogr. A 1191* (2008) 162–170. https://doi.org/10.1016/j.chroma.2008.01.061

M.F.C. Girard, P. Knight, R. Giles, G. Hopfgartner, Effects of the LC mobile phase in vacuum differential mobility spectrometry-mass spectrometry for the selective analysis of antidepressant drugs in human plasma, *Anal. Bioanal. Chem. 414* (2022) 7243–7252. https://doi.org/10.1007/s00216-022-04276-0

A. Gomez, K. Tang, Charge and fission of droplets in electrostatic sprays, *Phys. Fluids 6* (1994) 404–414. https://doi.org/10.1063/1.868037

V. González-Ruiz, A.I. Olives, M.A. Martín, Core-shell particles lead the way to renewing high-performance liquid chroma-tography, *Trends Anal. Chem. 64* (2015) 17–28. https://doi.org/10.1016/j.trac.2014.08.008

F. Gritti, M. F. Wahab, Understanding the science behind packing high-efficiency columns and capillaries: facts, fundamentals, challenges, and future directions, *LCGC North Am. 36* (2018) 82–98.

F. Gritti, T. McDonald, M. Gilar, Intrinsic advantages of packed capillaries over narrow-bore columns in very high-pressure gradient liquid chromatography, *J. Chromatogr. A 1451* (2016) 107–119. https://doi.org/10.1016/j.chroma.2016.05.035

G.J. Guimaraes, M.G. Bartlett, Managing nonspecific adsorption to liquid chromatography hardware: a review, *Anal. Chim. Acta 1250* (2023) 340994. https://doi.org/10.1016/j.aca.2023.340994

E.-M. Harrieder, F. Kretschmer, S. Böcker, M. Witting, Current state-of-the-art of separation methods used in LC-MS based metabolomics and lipidomics, *J. Chromatogr.y B 1188* (2022) 123069. https://doi.org/10.1016/j.jchromb.2021.123069

B. He, F. Regnier, Microfabricated liquid chromatography columns based on collocated monolith support structures, *J. Pharm. Biomed. Anal. 17* (1998) 925–932. https://doi.org/10.1016/S0731-7085(98)00060-0

B. He, X. Di, F. Guled, A.V.E. Harder, A.M.J.M. Van Den Maagdenberg, G.M. Terwindt, E.H.J. Krekels, I. Kohler, A. Harms, R. Ramautar, T. Hankemeier, Quantification of endocannabinoids in human cerebrospinal fluid using a novel micro-flow liquid chromatography-mass spectrometry method, *Anal. Chim. Acta 1210* (2022) 339888. https://doi.org/10.1016/j.aca.2022.339888

M. Hilhorst, C. Briscoe, N. Van De Merbel, Sense and nonsense of miniaturized LC–MS/MS for bioanalysis, *Bioanalysis 6* (2014) 3263–3265. https://doi.org/10.4155/bio.14.263

Y.M. Ibrahim, M.E. Belov, A.V. Liyu, R.D. Smith, Automated gain control ion funnel trap for orthogonal time-of-flight mass spectrometry, *Anal. Chem. 80* (2008) 5367–5376. https://doi.org/10.1021/ac8003488

Y. Ishihama, Proteomic LC–MS systems using nanoscale liquid chromatography with tandem mass spectrometry, *J. Chromatogr. A 1067* (2005) 73–83. https://doi.org/10.1016/j.chroma.2004.10.107

N. Ishizuka, H. Minakuchi, K. Nakanishi, N. Soga, H. Nagayama, K. Hosoya, N. Tanaka, Performance of a monolithic silica column in a capillary under pressure-driven and electrodriven conditions, *Anal. Chem. 72* (2000) 1275–1280. https://doi.org/10.1021/ac990942q

C. Jacquet, G. Hopfgartner, Microflow liquid chromatography coupled to mass spectrometry (μLC–MS) workflow for O-glycopeptides isomers analysis combining differential mobility spectrometry and collision induced and electron capture dissociation, *J. Am. Soc. Mass Spectrom. 33* (2022) 688–694. https://doi.org/10.1021/jasms.1c00381

H. Kafeenah, C.-M. Kuo, T.-Y. Chang, H.-H. Jen, J.-H. Yang, Y.-S. Shen, C.-H. Wu, S.-H. Chen, Label-free and de-conjugation-free workflow to simultaneously quantify trace amount of free/conjugated and protein-bound estrogen metabolites in human serum, *Anal. Chim. Acta 1232* (2022) 340457. https://doi.org/10.1016/j.aca.2022.340457

K.W. Kahl, J.Z. Seither, L.J. Reidy, LC-MS-MS vs ELISA: validation of a comprehensive urine toxicology screen by LC-MS-MS and a comparison of 100 forensic specimens, *J. Anal. Toxicol. 43* (2019) 734–745. https://doi.org/10.1093/jat/bkz066

M. Karas, U. Bahr, T. Dülcks, Nano-electrospray ionization mass spectrometry: addressing analytical problems beyond routine, *Fresenius' J Anal Chem366* (2000) 669–676. https://doi.org/10.1007/s002160051561

W. Kim, M. Guo, P. Yang, D. Wang, Microfabricated monolithic multinozzle emitters for nanoelectrospray mass spectrometry, *Anal. Chem. 79* (2007) 3703–3707. https://doi.org/10.1021/ac070010j

L. Konermann, E. Ahadi, A.D. Rodriguez, S. Vahidi, Unraveling the mechanism of electrospray ionization, *Anal. Chem. 85* (2013) 2–9. https://doi.org/10.1021/ac302789c

N.L. Kuehnbaum, P. Britz-McKibbin, New advances in separation science for metabolomics: resolving chemical diversity in a post-genomic era, *Chem. Rev. 113* (2013) 2437–2468. https://doi.org/10.1021/cr300484s

S.C. Lam, E. Sanz Rodriguez, P.R. Haddad, B. Paull, Recent advances in open tubular capillary liquid chromatography, *Analyst 144* (2019) 3464–3482. https://doi.org/10.1039/C9AN00329K

J. Lenčo, S. Jadeja, D.K. Naplekov, O.V. Krokhin, M.A. Khalikova, P. Chocholouš, J. Urban, K. Broeckhoven, L. Nováková, F. Švec, Reversed-phase liquid chromatography of peptides for bottom-up proteomics: a tutorial, *J. Proteome Res. 21* (2022) 2846–2892. https://doi.org/10.1021/acs.jproteome.2c00407

N. Li, T. Zhang, G. Chen, J. Xu, G. Ouyang, F. Zhu, Recent advances in sample preparation techniques for quantitative detection of pharmaceuticals in biological samples, *Trends Anal. Chem. 142* (2021) 116318. https://doi.org/10.1016/j.trac.2021.116318

T. Liang, P. Kebarle, Dependence of ion intensity in electrospray mass spectrometry on the concentration of the analytes in the electrosprayed solution, Anal. Chem. 65 (1993) 3654–3668. https://doi.org/10.1021/ac00072a020

B.L. Ling, W. Baeyens, C. Dewaele, Comparative study of "on-column focusing" applied to micro-LC and conventional LC, *J. Microcolumn Sep. 4* (1992) 17–22. https://doi.org/10.1002/mcs.1220040105

D. Liu, X. Han, X. Liu, M. Cheng, M. He, G. Rainer, H. Gao, X. Zhang, Measurement of ultra-trace level of intact oxytocin in plasma using SALLE combined with nano-LC–MS, *J. Pharm. Biomed. Anal. 173* (2019) 62–67. https://doi.org/10.1016/j.jpba.2019.04.023

R. Liu, Q. Li, L.M. Smith, Detection of large ions in time-of-flight mass spectrometry: effects of ion mass and acceleration voltage on microchannel plate detector response, *J. Am. Soc. Mass Spectrom. 25* (2014) 1374–1383. https://doi.org/10.1007/s13361-014-0903-2

A. Lubin, S. Sheng, D. Cabooter, P. Augustijns, F. Cuyckens, Flexible nano- and microliter injections on a single liquid chromatography–mass spectrometry system: minimizing sample preparation and maximizing linear dynamic range, *J. Chromatogr. A 1524* (2017) 101–107. https://doi.org/10.1016/j.chroma.2017.09.053

M. Majewsky, D. Castel, L. Le Dret, P. Johann, D.T. Jones, S.M. Pfister, W.E. Haefeli, J. Burhenne, Systematic identification of suspected anthelmintic benzimidazole metabolites using LC–MS/MS, *J. Pharm. Biomed. Anal. 151* (2018) 151–158. https://doi.org/10.1016/j.jpba.2017.12.056

S.N. Majuta, A. DeBastiani, P. Li, S.J. Valentine, Combining field-enabled capillary vibrating sharp-edge spray ionization with microflow liquid chromatography and mass spectrometry to enhance 'omics analyses, *J. Am. Soc. Mass Spectrom. 32* (2021) 473–485. https://doi.org/10.1021/jasms.0c00376

P. Mao, H.-T. Wang, P. Yang, D. Wang, Multinozzle emitter arrays for nanoelectrospray mass spectrometry, *Anal. Chem. 83* (2011) 6082–6089. https://doi.org/10.1021/ac2011813

I. Marginean, R.T. Kelly, D.C. Prior, B.L. LaMarche, K. Tang, R.D. Smith, Analytical characterization of the electrospray ion source in the nanoflow regime, *Anal. Chem. 80* (2008) 6573–6579. https://doi.org/10.1021/ac800683s

E.J. Maxwell, X. Zhong, D.D.Y. Chen, Asymmetrical emitter geometries for increased range of stable electrospray flow rates, *Anal. Chem. 82* (2010) 8377–8381. https://doi.org/10.1021/ac1017953.

P.J. McClory, K. Håkansson, Corona discharge suppression in negative ion mode nanoelectrospray ionization via trifluoroethanol addition, *Anal. Chem. 89* (2017) 10188–10193. https://doi.org/10.1021/acs.analchem.7b01225

K. Mejía-Carmona, J. Soares Da Silva Burato, J.V.B. Borsatto, A.L. De Toffoli, F.M. Lanças, Miniaturization of liquid chromatography coupled to mass spectrometry, *Trends Anal. Chem. 122* (2020) 115735. https://doi.org/10.1016/j.trac.2019.115735

M.K. Midha, C. Kapil, M. Maes, D.H. Baxter, S.R. Morrone, T.J. Prokop, R.L. Moritz, Vacuum insulated probe heated electrospray ionization source enhances microflow rate chromatography signals in the Bruker timsTOF mass spectrometer, *J. Proteome Res. 22* (2023) 2525–2537. https://doi.org/10.1021/acs.jproteome.3c00305

H. Minakuchi, K. Nakanishi, N. Soga, N. Ishizuka, N. Tanaka, Octadecylsilylated porous silica rods as separation media for reversed-phase liquid chromatography, *Anal. Chem. 68* (1996) 3498–3501. https://doi.org/10.1021/ac960281m

D. Moravcová, P. Jandera, J. Urban, J. Planeta, Characterization of polymer monolithic stationary phases for capillary HPLC,

J. Sep. Sci. 26 (2003) 1005–1016. https://doi.org/10.1002/jssc.200301498

J.C. Nadal, F. Borrull, R.M. Marcé, N. Fontanals, Novel in-house mixed-mode ion-exchange materials for sorptive phase extraction techniques, *Adv. Sample Preparation 1* (2022) 100008. https://doi.org/10.1016/j.sampre.2022.100008

C.E.D. Nazario, M.R. Silva, M.S. Franco, F.M. Lanças, Evolution in miniaturized column liquid chromatography instrumentation and applications: an overview, *J. Chromatogr. A 1421* (2015) 18–37. https://doi.org/10.1016/j.chroma.2015.08.051

S.K. Neef, U. Hofmann, T.E. Mürdter, M. Schwab, M. Haag, Performance comparison of narrow-bore and capillary liquid-chromatography for non-targeted metabolomics profiling by HILIC-QTOF-MS, *Talanta 260* (2023) 124578. https://doi.org/10.1016/j.talanta.2023.124578

E. Olesti, V. González-Ruiz, M.F. Wilks, J. Boccard, S. Rudaz, Approaches in metabolomics for regulatory toxicology applications, *Analyst 146* (2021) 1820–1834. https://doi.org/10.1039/D0AN02212H

C. Orlandi, C. Jacques, H. Duplan, L. Debrauwer, E.L. Jamin, Miniaturized two-dimensional heart cutting for LC–MS-based metabolomics, *Anal. Chem. 95* (2023) 2822–2831. https://doi.org/10.1021/acs.analchem.2c04196

S. Perchepied, H. Ritchie, G. Desmet, S. Eeltink, Insights in column packing processes of narrow bore and capillary-scale columns: Methodologies, driving forces, and separation performance—a tutorial review, *Anal. Chim. Acta 1235* (2022) 340563. https://doi.org/10.1016/j.aca.2022.340563

R. S. Plumb, G. J. Dear, D. Mallett, I. J. Fraser, J. Ayrton, C. Ioannou, The application of fast gradient capillary liquid chromatography/mass spectrometry to the analysis of pharmaceuticals in biofluids, *Rapid Commun. Mass Spectrom. 13* (1999) 865–872.

H. Poppe, Some reflections on speed and efficiency of modern chromatographic methods, *J. Chromatogr. A 778* (1997) 3–21. https://doi.org/10.1016/S0021-9673(97)00376-2

G.R.D. Prabhu, V.K. Ponnusamy, H.A. Witek, P.L. Urban, Sample flow rate scan in electrospray ionization mass spectrometry reveals alterations in protein charge state distribution, *Anal. Chem. 92* (2020) 13042–13049. https://doi.org/10.1021/acs.analchem.0c01945

A. Premstaller, H. Oberacher, W. Walcher, A.M. Timperio, L. Zolla, J.-P. Chervet, N. Cavusoglu, A. Van Dorsselaer, C.G. Huber, High-performance liquid chromatography−electrospray ionization mass spectrometry using monolithic capillary columns for proteomic studies, *Anal. Chem. 73* (2001) 2390–2396. https://doi.org/10.1021/ac010046q

A. Prüß, C. Kempter, J. Gysler, T. Jira, Extracolumn band broadening in capillary liquid chromatography, *J. Chromatogr. A 1016* (2003) 129–141. https://doi.org/10.1016/S0021-9673(03)01290-1

B.R. Reschke, A.T. Timperman, A study of electrospray ionization emitters with differing geometries with respect to flow rate and electrospray voltage, *J. Am. Soc. Mass Spectrom. 22* (2011) 2115–2124. https://doi.org/10.1007/s13361-011-0251-4

B. Rochat, P. Waridel, J. Barblan, P.-E. Sottas, M. Quadroni, Robust and sensitive peptidomics workflow for plasma based on specific extraction, lipid removal, capillary LC setup and multinozzle ESI emitter, *Talanta 223* (2021) 121617. https://doi.org/10.1016/j.talanta.2020.121617

M. Rogeberg, H. Malerod, H. Roberg-Larsen, C. Aass, S.R. Wilson, On-line solid phase extraction–liquid chromatography, with emphasis on modern bioanalysis and miniaturized systems, *J. Pharm. Biomed. Anal. 87* (2014) 120–129. https://doi.org/10.1016/j.jpba.2013.05.006

G. Rozing, Micropillar array columns for advancing nanoflow HPLC, *Microchem. J. 170* (2021) 106629. https://doi.org/10.1016/j.microc.2021.106629

Y. Saito, K. Jinno, T. Greibrokk, Capillary columns in liquid chromatography: between conventional columns and micro-chips, *J. Sep. Sci. 27* (2004) 1379–1390. https://doi.org/10.1002/jssc.200401902

B.B. Schneider, H. Javaheri, L. Bedford, T.R. Covey, Sampling efficiency improvement to an electrospray ionization mass spectrometer and its implications for liquid chromatography based inlet systems in the nanoliter to milliliter per minute flow range, *J. Am. Soc. Mass Spectrom. 32* (2021) 1441–1447. https://doi.org/10.1021/jasms.1c00053

S. Seidi, M. Tajik, M. Baharfar, M. Rezazadeh, Micro solid-phase extraction (pipette tip and spin column) and thin film solid-phase microextraction: miniaturized concepts for chromatographic analysis, *Trends Anal. Chem. 118* (2019) 810–827. https://doi.org/10.1016/j.trac.2019.06.036

J. Šesták, D. Moravcová, V. Kahle, Instrument platforms for nano liquid chromatography, *J. Chromatogr. A 1421* (2015) 2–17. https://doi.org/10.1016/j.chroma.2015.07.090

Y. Shen, T.A. Van Beek, H. Zuilhof, B. Chen, Hyphenation of optimized microfluidic sample preparation with nano liquid chromatography for faster and greener alkaloid analysis, *Anal. Chim. Acta 797* (2013) 50–56. https://doi.org/10.1016/j.aca.2013.08.034

M. Shipkova, D. Svinarov, LC–MS/MS as a tool for TDM services: where are we?, *Clin. Biochem. 49* (2016) 1009–1023. https://doi.org/10.1016/j.clinbiochem.2016.05.001

S. Souverain, S. Rudaz, J. Veuthey, Matrix effect in LC-ESI-MS and LC-APCI-MS with off-line and on-line extraction procedures, *J. Chromatogr. A 1058* (2004) 61–66. https://doi.org/10.1016/S0021-9673(04)01477-3

D. Spaggiari, S. Fekete, P.J. Eugster, J.-L. Veuthey, L. Geiser, S. Rudaz, D. Guillarme, Contribution of various types of liquid chromatography–mass spectrometry instruments to band broadening in fast analysis, *J. Chromatogr. A 1310* (2013) 45–55. https://doi.org/10.1016/j.chroma.2013.08.001

T. Strmeň, V. Vrkoslav, O. Pačes, J. Cvačka, Evaluation of an ion source with a tubular nebulizer for microflow atmospheric pressure chemical ionization, *Monatsh Chem. 149* (2018) 987–994. https://doi.org/10.1007/s00706-018-2172-4

F. Svec, Monolithic columns: a historical overview, *Electrophoresis 38* (2017) 2810–2820. https://doi.org/10.1002/elps.201700181

F. Svec, Y. Lv, Advances and recent trends in the field of monolithic columns for chromatography, *Anal. Chem. 87* (2015) 250–273. https://doi.org/10.1021/ac504059c

J.E.P. Syka, J.A. Marto, D.L. Bai, S. Horning, M.W. Senko, J.C. Schwartz, B. Ueberheide, B. Garcia, S. Busby, T. Muratore, J. Shabanowitz, D.F. Hunt, Novel linear quadrupole ion trap/FT mass spectrometer: performance characterization and use in the comparative analysis of

histone h3 post-translational modifications, *J. Proteome Res. 3* (2004) 621–626. https://doi.org/10.1021/pr0499794

N. Tanaka, D.V. McCalley, Core–shell, ultrasmall particles, monoliths, and other support materials in high-performance liquid chromatography, *Anal. Chem. 88* (2016) 279–298. https://doi.org/10.1021/acs.analchem.5b04093

D. Thomas, M. Eberle, S. Schiffmann, D.D. Zhang, G. Geisslinger, N. Ferreirós, Nano-LC–MS/MS for the quantitation of ceramides in mice cerebrospinal fluid using minimal sample volume, *Talanta 116* (2013) 912–918. https://doi.org/10.1016/j.talanta.2013.07.057

S. Thurmann, C. Lotter, J.J. Heiland, B. Chankvetadze, D. Belder, Chip-based high-performance liquid chromatography for high-speed enantioseparations, *Anal. Chem. 87* (2015) 5568–5576. https://doi.org/10.1021/acs.analchem.5b00210

K.K. Unger, R. Skudas, M.M. Schulte, Particle packed columns and monolithic columns in high-performance liquid chromatography-comparison and critical appraisal, *J. Chromatogr. A 1184* (2008) 393–415. https://doi.org/10.1016/j.chroma.2007.11.118

J. Urban, P. Jandera, Polymethacrylate monolithic columns for capillary liquid chromatography, *J. Sep. Sci. 31* (2008) 2521–2540. https://doi.org/10.1002/jssc.200800182

W.D. Van Dongen, W.M. Niessen, LC–MS systems for quantitative bioanalysis, *Bioanalysis 4* (2012) 2391–2399. https://doi.org/10.4155/bio.12.221

K. Vanderlinden, K. Broeckhoven, Y. Vanderheyden, G. Desmet, Effect of pre- and post-column band broadening on the performance of high-speed chromatography columns under isocratic and gradient conditions, *J. Chromatogr. A 1442* (2016) 73–82. https://doi.org/10.1016/j.chroma.2016.03.016

B. Vankeerberghen, J. Op De Beeck, G. Desmet, On-chip comparison of the performance of first- and second-generation micropillar array columns, *Anal. Chem. 95* (2023) 13822–13828. https://doi.org/10.1021/acs.analchem.3c01829

J.P.C. Vissers, H.A. Claessens, C.A. Cramers, Microcolumn liquid chromatography: instrumentation, detection and applications, *J. Chromatogr. A 779* (1997) 1–28. https://doi.org/10.1016/S0021-9673(97)00422-6.

J.P.C. Vissers, A.H. De Ru, M. Ursem, J.-P. Chervet, Optimised injection techniques for micro and capillary liquid chromatography, *J. Chromatogr. A 746* (1996) 1–7. https://doi.org/10.1016/0021-9673(96)00322-6

E.J. Want, P. Masson, F. Michopoulos, I.D. Wilson, G. Theodoridis, R.S. Plumb, J. Shockcor, N. Loftus, E. Holmes, J.K. Nicholson, Global metabolic profiling of animal and human tissues via UPLC-MS, *Nat. Protoc. 8* (2013) 17–32. https://doi.org/10.1038/nprot.2012.135

T. Werres, T.C. Schmidt, T. Teutenberg, The influence of injection volume on efficiency of microbore liquid chromatography columns for gradient and isocratic elution, *J. Chromatogr. A* 2021 (*1641*) 461965. https://doi.org/10.1016/j.chroma.2021.461965

A. Westman, G. Brinkmalm, D.F. Barofsky, MALDI induced saturation effects in chevron microchannel plate detectors, *Int. J. Mass Spectrom. Ion Processes 1169–170* (1997) 79–87. https://doi.org/10.1016/S0168-1176(97)00205-X

J. Xiao, J. Shi, R. Li, L. Her, X. Wang, J. Li, M.J. Sorensen, V. Bhatt-Mehta, H.-J. Zhu, Developing a SWATH capillary LC-MS/MS method for simultaneous therapeutic drug monitoring and untargeted metabolomics analysis of neonatal plasma, *J. Chromatogr. B 1179* (2021) 122865. https://doi.org/10.1016/j.jchromb.2021.122865

H. Yin, K. Killeen, The fundamental aspects and applications of Agilent HPLC-Chip, *J. Sep. Sci. 30* (2007) 1427–1434. https://doi.org/10.1002/jssc.200600454

E.M. Yuill, N. Sa, S.J. Ray, G.M. Hieftje, L.A. Baker, Electrospray ionization from nanopipette emitters with tip diameters of less than 100 nm, *Anal. Chem. 85* (2013) 8498–8502. https://doi.org/10.1021/ac402214g

A. Zardini Buzatto, B.K. Kwon, L. Li, Development of a NanoLC-MS workflow for high-sensitivity global lipidomic analysis, *Anal. Chim. Acta 1139* (2020) 88–99. https://doi.org/10.1016/j.aca.2020.09.001

Studies of athlete biological passport biomarkers and clinical parameters in male and female users of anabolic androgenic steroids and other doping agents

Annica Börjesson[1,3] 🟢 | Mikael Lehtihet[4] | Alexander Andersson[2,3] |
Marja-Liisa Dahl[1,3] | Veronica Vicente[5,6] | Magnus Ericsson[1,2,3] | Lena Ekström[1] 🟢

[1]Division of Clinical Pharmacology, Department of Laboratory Medicine, Karolinska Institutet, Stockholm, Sweden

[2]Anti-Doping Laboratory, Clinical Pharmacology, Karolinska University Laboratory, Karolinska University Hospital, Stockholm, Sweden

[3]Clinical Pharmacology, Karolinska University Laboratory, Karolinska University Hospital, Stockholm, Sweden

[4]Department of Medicine, Karolinska Institutet and St Görans Hospital, Stockholm, Sweden

[5]Ambulance Medical Service in Stockholm [Ambulanssjukvården i Storstockholm AB], Academic EMS, Stockholm, Sweden

[6]Department of Clinical Science and Education, Karolinska Institutet, Stockholm, Södersjukhuset, Stockholm, Sweden

Correspondence
Annica Börjesson, Division of Clinical Pharmacology C1-68 Department of Laboratory Medicine, Karolinska Institutet, Karolinska University Hospital, Huddinge 141 86, Stockholm, Sweden.
Email: annica.borjesson@ki.se

Abstract

The use of anabolic androgenic steroids (AAS) and other performance enhancing substances can change over time, so there is a need to constantly update what substances are used and can be detected. Six women and 30 men anabolic androgenic steroid users were recruited who filled out an anonymous questionnaire about their use of performance enhancing substances during the past year. Sampling took place on a single occasion and included blood and urine collection. Our aim was to identify which doping agents can be detected in men and women self-reporting AAS use. The first choice of substances differed between men (testosterone) and women (oxandrolone). The use of growth hormones was reported among men (10%) and women (50%). Growth hormone releasing factors/secretagogs were reported by about ~ 20% in both genders. Nandrolone was the most frequently detected anabolic androgenic steroid even in those who did not report use in the past year. Of the current male testosterone users, 82% exhibited testosterone/epitestosterone (T/E) ratios of > 4. Men with current testosterone use displayed 4-fold and 6-fold higher median T/E, respectively, when compared with recent and previous testosterone users (P = 0.0001). Dermal testosterone use in women (n = 2) was not associated with a T/E ratio of > 4, but with supra-physiological total serum testosterone concentrations. Changes in gonadotropins and hematological parameters were associated with the time of the last anabolic androgenic steroid intake in men, whereas in women these biomarkers were within the normal range. This highlights gender specific differences and indicates the need for additional biomarkers in female athletes.

KEYWORDS
anabolic androgenic steroids, athlete biological passport, doping tests, testosterone, urinary steroid profile

1 | INTRODUCTION

Anabolic androgenic steroids (AAS) are used both in elite and recreational athletes and considered to be a public health problem and a concern to society.[1-3] Users of AAS are motivated by gaining a larger muscle mass, a greater physical appearance, and muscle strength.[4,5] The great majority of users are male.[4] AAS are commonly used in doses up to 50–100 times higher than those used for medical replacement therapy.[6] AAS users, both men[7] and women,[4] consistently combine other drugs with different types of AAS. These include other performance enhancing substances (PES) often used to attenuate the AAS induced side effects, i.e. aromatase inhibitors and stimulants. Even though AAS use is not a new phenomenon, the practice concerning the substances and doses used may change over time, and hence, there is a need for continuous knowledge updates.

The detection of AAS is important for fair play, for health protection, and as a deterrent.[8] In competitive elite sport, testing is organized by the World Anti-Doping Agency (WADA), with accredited laboratories world-wide. The detection of exogenous steroids is performed by mass spectrometry to analyze synthetic steroids and/or their metabolites in urine. The detection of endogenous anabolic androgenic steroids (EAAS) intake, i.e. testosterone (T), is based on longitudinal monitoring of the urinary steroid metabolite ratios including the testosterone to epitestosterone (E) ratio, the androsterone (A) to etiocholanolone (Etio) ratio, the 5α-androstane-3α,17β-diol (5αAdiol) to epitestosterone ratio, the 5αAdiol to 5β-androstane-3α,17β-diol (5βAdiol) ratio and the A/T ratio in the steroidal module of the athlete biological passport (ABP).[9] The steroid module of ABP alone is seldom used to judge an athlete as positive for endogenous anabolic androgenic steroids, instead a confirmatory method based on gas chromatography–combustion–isotope ratio mass spectrometry (GC-C-IRMS) is used.[10] In athletes not previously tested and in forensic samples, population-based cut-offs are used, i.e. a T/E ratio of 4 being indicative of exogenous testosterone use. The T/E ratio is associated with a deletion polymorphism in glucuronosyl transferase 2B17 (UGT2B17). Individuals devoid of the UGT2B17 gene (del/del) excrete negligible amounts of testosterone in the urine and rarely reach the T/E cut-off value of 4 after testosterone doping.[11] Notably, the urinary T/E ratio was not sensitive when supra-physiological serum testosterone concentrations were detected in female athletes, most likely induced by testosterone intake.[12] Therefore, it may be informative to include longitudinal serum testosterone levels in the ABP in the future. Monitoring steroid hormones, e.g. dihydrotestosterone (DHT), in serum has been discussed since it has been shown to increase the likelihood of detecting doping with endogenous steroids in men.[13]

Luteinizing hormone (LH), follicle stimulating hormone (FSH), and hemoglobin (HB) are well established biomarkers affected by AAS abuse. They can be used in health care to get an indication of whether a person is using AAS.[14,15] Moreover, it is well known that AAS disturb the cholesterol profile, with an increase in LDL and apolipoprotein B (ApoB).[16] High total cholesterol levels and hematocrit are cardiovascular risk factors for atherosclerosis and thrombotic events in steroid users.[17]

The aim of this study was to employ doping analyses, performed as required by WADA, in male and female volunteers with current, recent, or previous AAS use and to relate the results with the information provided by the subjects concerning their AAS use pattern. Moreover, hematological parameters, cholesterol profile, and endocrine status were determined and analyzed in relation to the time of the last AAS intake.

2 | MATERIAL AND METHODS

2.1 | Data collection and study population

Thirty men and six women between 21–66 years of age (Table 1) were recruited to the study between October 2016 and December 2017. Individuals using performance enhancing substances during the past year were asked to participate in the study. Recruitment was performed through the Anti-Doping Hot-Line, Karolinska University Hospital, Stockholm, Sweden. The Anti-Doping Hot-Line was established in 1993 as an anonymous free telephone counseling service for people concerned about or affected by their non-medical use of AAS.[1] "Snowball sampling", a method for studying hard-to-reach populations, was used for enrolment. This method introduced by Goodman,[18] implies that an initial contact generates new contacts and thus the sample size grows like a rolling snowball. Participation was commenced after oral and written informed consent and the study was approved by the Ethics Review Board in Stockholm. Sampling took place on one single occasion and included the collection of blood (EDTA and serum) and urine. Height and body weight were recorded at the study visit and the participants were informed of the risks of substance abuse. The participants sat down for at least

TABLE 1 Demographic data of the participants. The data are given as median and ranges

	Men (n = 30)	Women (n = 6)
Age (years)	33 (21–66)	34 (21–54)
AAS debut age (years)	26 (16–52)	27 (19–50)
AAS duration (years)	4 (0.5–30)	2.5 (0.5–10)
Number of AAS cycles (last year)	2 (1–3)	2 (1–3)
Number of AAS substances per cycle (last year)	3 (1–7)	2 (1–6)
Systolic blood pressure, mmHg	178 (158–200)	184 (176–193)
Diastolic blood pressure, mmHg	88 (58–128)	97 (83–117)
Length (cm)	179 (172–200)	164 (158–173)
Body weight (kg)	91 (80–128)	71 (58–83)
BMI[1]	28.4 (22.8–34.6)	26.1 (22.3–29.6)

[1]Definition Body Mass Index $(BMI) = \frac{weight\ (kg)}{length \times length\ (m2)} = \frac{kg}{m2}.$

10 minutes prior to blood pressure measurements and blood sampling. Blood pressure was measured by a study nurse according to Swedish clinical guidelines. No financial remuneration was given to the participants.

2.2 | Questionnaire

The participants filled out an anonymous questionnaire about their use of performance enhancing substances as well as all other drugs (including pharmaceutical drugs). The information requested was: age, gender, and number of years that they had used PES. The participants were further asked about used substances, doses, lengths of cycles, and the number of different AAS intakes per year.

2.3 | Sample analysis

Performance enhancing substances were analyzed in urine by the WADA Accredited Anti-Doping Laboratory at the Department of Clinical Pharmacology, Karolinska University Laboratory, Stockholm. Endogenous steroids were analyzed using GC–MS/MS according to WADA TD2016EAAS[19] as described previously.[20] Exogenous steroids and other PES were screened with GC–MS/MS and LC–MS/MS according to WADA TD2018MRPL[21] (non-threshold substances) and TD2018DL[22] (threshold substances).

Whole blood samples were collected in EDTA tubes and analyzed according to WADA Athlete Biological Passport Operating Guidelines. All samples were analyzed within 8 hours and if not analyzed within 2 hours the samples were stored at 4°C (i.e. all samples displayed a blood stability score well below 85) using Sysmex XN-1000 for hemoglobin, hematocrit (HCT), red blood cell count (RBC), mean corpuscular volume (MCV), mean corpuscular hemoglobin (MCH), mean corpuscular hemoglobin concentration (MCHC), reticulocyte percentage, reticulocyte numbers, and immature reticulocyte fraction (IRF).

Whole blood samples were collected in serum tubes and serum was obtained within 4 hours by spinning the tubes for 10 minutes at $2000 \times g$ and stored immediately at $-80°C$ prior to analyses. Testosterone, sex hormone-binding globulin (SHBG), LH, and FSH were determined with ISO 15189:2012 accredited methods at Clinical Chemistry, Karolinska University Laboratory. Total serum testosterone was measured using chemiluminescent technology UniCel® DxI 800 Immunoassay System and Access Testosterone Reagent Packs (Cat #33560) from Beckman Coulter (Brea, CA, USA). Luteinizing hormone and follicle stimulating hormone were determined with an Auto-DELFIA instrument and 2-site immunoradiometric assays using kits (PN: B017–201 and B031–101) from PerkinElmer (PerkinElmer Life and Analytical Sciences, Turku, Finland).

Serum concentrations of dihyrdotestosterone and testosterone, as well as the sulfate (S) and glucuronide (G) conjugates were analyzed by ultra-high performance liquid chromatography coupled to high resolution mass spectrometric detection (UHPLC-HRMS) as described.[23] Briefly, the analytes were extracted from serum samples using solid phase extraction with HLB cartridges for purification and pre-concentration of the analytes. The developed method included chromatographic separation of the analytes using a YMC-Triart C18 column 100×2.0 mm with 1.9 μm particles with a precolumn YMC-Triart C18 5×2.1 mm (YMC Co. Ltd, Kyoto, Japan). Gradient elution was applied using a mobile phase consisting of: (A) 10 mM ammonium acetate adjusted to pH 9.5 using 20% ammonium hydroxide, and (B) 10 mM ammonium acetate adjusted to pH 9.5 and methanol (10: 90% v/v). The gradient LC run had an initial composition of 50% B for 0.20 min followed by 65% B for 4.8 min, and finally 100% B for 8 min. The composition of 100% B was held for 9.6 min then decreased linearly to 50% B for 9.7 min. Equilibration between runs was set for 2.3 min (total run time 12 min).

The mass spectrometric detection was set to acquire ion signals during the run time 0.5–9.5 min and operating in both negative and positive electrospray ionization (ESI) modes. Two scan ranges were adopted according to the targeted analyte's detection mode. Scan ranges (300–500 m/z) and (200–400 m/z) were selected in the negative and positive ESI modes, respectively. The mass spectrometer was operating in full scan mode with a resolution of 70,000. The limit of detection for testosterone and dihydrotestosterone were 0.009 ng/mL and 0.036 ng/mL, respectively.

Growth hormone (GH) was analyzed with the GH isoform test as described previously.[24] The GH releasing peptides/secretagogs were analyzed according to TD2018MRPL.[21]

2.4 | UGT2B17 genotyping

The UGT2B17 insertion/deletion polymorphism was genotyped using a premade copy number assay (#Hs03185327_cn, Life Technologies). The ubiquitously expressed RNase P (#4403326, Control Reagents, Life Technologies) gene was used as the endogenous reference gene for reaction quality control. Briefly, the PCR was carried out in a 15 μL volume including 2 μL genomic DNA, and 2× TaqMan Universal Master Mix II (#4440043, Applied Biosystems). Samples with RNase P signals but no UGT2B17 amplification were identified as del/del. The del/del genotypes were replicated and confirmed in two separate experiments. No discrimination between UGT2B17 allele-carriers (ins/ins and ins/del) was performed.

2.5 | Statistical and data analysis

The results are presented as the median with the ranges in parenthesis if not stated otherwise. The distribution was tested by the Kolmogorov–Smirnov test, and none of the parameters passed the normality test (or were too few to allow testing). One-way non-parametric ANOVA (Kruskal Wallis) followed by Dunn's test were used to compare the ABP ratios, cardiovascular and endocrine biomarkers between groups. For comparison of the median values of two groups the Mann Whitney test was used. Spearman's rank correlation test was employed for correlation analysis. The significance level was

set at $P = 0.05$. Statistical analyses were performed using GraphPrism Software version 6 from GraphPad (San Diego, CA, USA).

3 | RESULTS

3.1 | Demographic data and screening test results

Demographic data of the participants are presented in Table 1.

Of the participants 83% were male and 17% were female. The participants were divided into three groups based on their last intake of anabolic androgenic steroids: current (within past 2 months); recent (2–6 months ago), and previous (6–12 months ago). Four women (67%) and 16 men (53%) reported a current AAS use, two women (33%) and nine men (30%) reported a recent use and five men (17%) reported a previous use. A current use of dietary supplements was reported by 36% of the participants. Eighty-three percent practiced stacking, i.e. used several different AAS agents and in cycles (periods of use and non-use). Sixteen men and one woman were using AAS continuously.

3.2 | Self-reported AAS substances

The most common AAS substance reported in women was oxandrolone followed by stanozolol and testosterone, whereas in men testosterone was the most popular steroid, followed by trenbolone and drostanolone, see Figure 1.

Of the 24 male testosterone users, only two reported the use of testosterone gel, and these two also used injectable testosterone compounds. The different injectable testosterone esters used consisted of testosterone enanthate (n = 20) and testosterone propionate (n = 4). Of the females using testosterone, two reported a current use of testosterone gel (10 and 20 mg/day, respectively), and one reported a previous use of testosterone enanthate (injection).

Detailed information was collected about the participant's AAS-schedules (substances, doses, and cycles). Weekly and daily doses were calculated by taking the total used amount of AAS in milligrams of each substance during the last cycle and dividing it by the number of weeks/days of the cycle. Men used higher doses (median 1368 mg/week, range 250–3800) than women (median 187 mg/week, range 70–900), P 0.0036. The weekly total doses of AAS are shown in Figure 2 and the daily doses are summarized in the supplementary file.

### 3.3 | Doping test results in relation with self-reported AAS use

The distributions of the positive tests are shown in Figure 3. Nandrolone and drostanolone were the most commonly detected steroids in subjects who *did not* report such use within the past year. Stanozolol and oxandrolone were the AAS detected in most of the participants reporting such use within the past 6 months.

### 3.4 | Urinary steroid profile in relation to testosterone intake, gender and UGT2B17 genotype

Eleven of the reported 27 T users had a positive urine test based on the urinary testosterone/epitestosterone ratio (T/E 4) and of those nine reported current testosterone use. The other two individuals reported an intake 2–6 months (T/E = 12.5) and 6–12 months ago (T/E = 5.2), respectively.

The men with a current use displayed 4-fold and 6-fold higher median T/E, respectively, compared with those reporting intake within the past year or no reported intake, $P = 0.0001$ (Figure 4A). For the other ABP ratios (A/T, A/etio, 5αAdiol/5βAdiol, 5αAdiol/E) no statistically significant differences between the participants with a current testosterone use and previous use were observed, Figure 4B-4E.
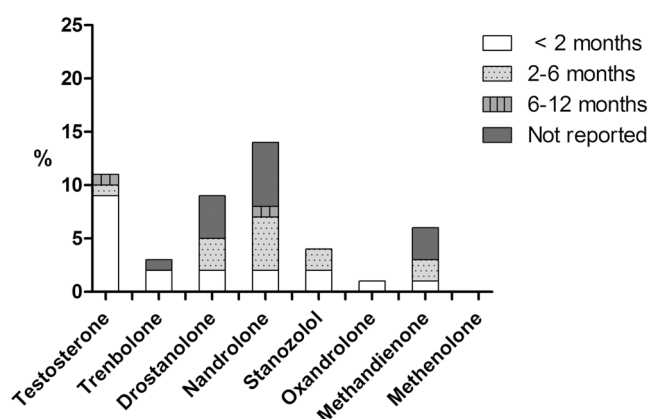
When comparing the ABP ratios in the male participants with females, significant differences were noted for the T/E ratio, whereas
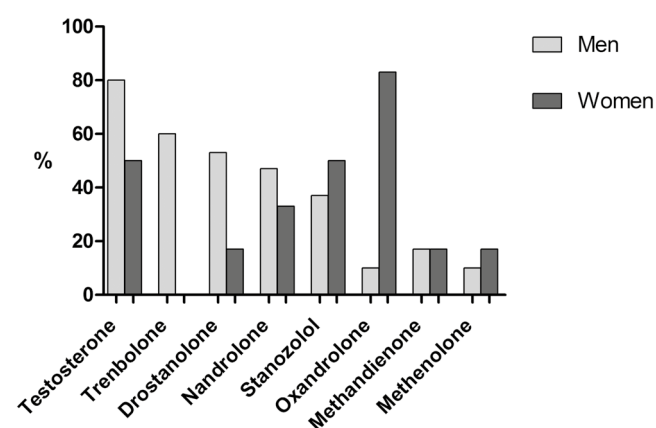
FIGURE 1 The most commonly reported AAS substances in men and women
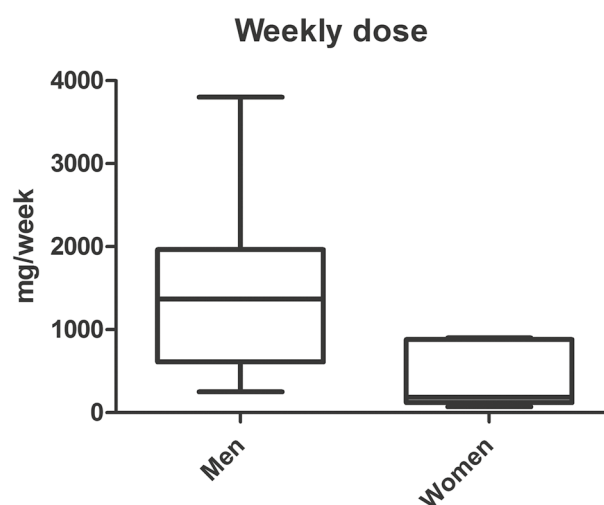
FIGURE 2 Boxplot of reported weekly doses in mg/week in men and women $P < 0.01$**

FIGURE 3 The number (%) of positive urine tests in relation to the last intake according to the self-reporting questionnaires

no gender differences in the other ABP ratios were found. Notably the two women with a current testosterone gel use exhibited T/E ratios of < 4 (2.4 and 0.6, respectively). Neither of the women's steroid profiles were suspicious following the criteria set by WADA (TD2016EAAS) but due to low numbers no statistical analyses were conducted.

Of the 30 male participants, three (10%) were found to be homozygous for the UGT2B17 deletion polymorphism (del/del) genotype. None of the female participants displayed the del/del genotype. One of the males with the del/del genotype reported a current testosterone enanthate intake and had a T/E ratio of 4.1, whereas the del/del males with a previous testosterone use had T/E ratios of 2.4 and 0.14.

3.5 | Detection of other doping substances

Peptide hormones and growth factors (S2) were analyzed only in individuals reporting current or a recent use within the past 2 months. Use of recGH was more commonly reported among women (50%) than in men (10%) (OR = 6.8; CI; 1.0–46.8, P = 0.03), and women reported doses of 1–6 IU/day and men 1–7 IU/day. The serum samples from participants with a current recGH use were analyzed with the Isoform GH test but all returned negative results (data not shown). Seven participants (six men, one woman) reported the use of GH releasing factors/secretagogs (Triptorelin, GHRP-2, ibutamoren, and ipamorelin) of which two reported use within the past 2 months. The individual reporting ibutamoren was tested positive on ibutamoren, even though the last intake of nasal droplets had taken place 8 weeks earlier.

Doping substances not belonging to class 1 and 2 (S1 and S2) on the prohibited WADA list[25] show that hormone and metabolic modulators (S4) and stimulants (S6) were detected in 39% and 27% of the samples, respectively. Diuretics (S5), cannabinoids (S8), and glucocorticoids (S9) were detected in <10% of the samples. Beta-agonists (S3) and narcotics (S7) were not detected in any of the participants.

3.6 | Cardiovascular and endocrine biomarkers

Of the hematological parameters normally included in the hematological module of athlete biological passport, hemoglobin, hematocrit, and reticulocyte % data for men are shown in Table 2. The men with a current AAS use displayed higher hemoglobin and hematocrit than those with a recent or previous use (borderline significance). No differences between the other hematological parameters (RBC, MCV, MCH, MCHC, IRF) analyzed were seen (data not shown). Of the lipoproteins determined, ApoA1 was the only lipid that differed between the groups, being highest in those with reported use 6–12 months earlier. In men, LH and FSH increased gradually with cessation time.

Due to the small number of female participants, individual data are presented in Table 3. Testosterone was quantified in women by both RIA and LC/MSMS. The methods showed a strong correlation (Rs = 0.98, P = 0.0003), with significantly higher total testosterone concentrations with RIA (median 2.5 nmol/L) than with LC–MS/MS (median 0.26 nmol/L), P = 0.03.

In addition to testosterone its metabolite dihydrotestosterone was also quantified with UHPLC-HRMS as the sulfate conjugate (DHTS), the main DHT form in the circulation. The women with current testosterone gel use showed higher serum testosterone (9.9 and 1.7 nmol/L) and DHTS (560 and 275 ng/mL) concentrations compared with non-testosterone users (T-range < 0.1–0.29 nmol/L and DHTS-range 19–237 ng/mL). Due to the low numbers, no statistical analyses were conducted for females.

4 | DISCUSSION

The results indicated that dermal testosterone use in women is not detectable with the traditional T/E biomarker, despite supraphysiological total testosterone serum concentrations. This is in line with a recent publication showing that elevated serum testosterone concentrations in two elite female athletes did not result in elevated urinary T/E ratios in their ABPs.[12] Since our study and the study conducted by Handelsman et al are both based on case observations, there is an urgent need to perform a controlled study in relation to transdermal testosterone administration in women. It is possible that longitudinal monitoring of the ABP biomarkers in our participants rather than single urine sampling would have resulted in atypical findings. It has been shown that the implementation of ABP has increased the probability of detecting testosterone gel use in men.[26,27] It is known that basal T/E ratios are higher in men than in women[28] and that the administration of intramuscular testosterone enanthate affects the T/E ratio to a larger degree in men than in women.[11,29]

There were no significant differences in the other ABP ratios in relation to the time of the last testosterone application consistent with the conclusion that T/E is the major ratio that triggers a confirmatory GC-C-IRMS analysis. In UGT2B17 del/del men, 5aAdiol/E ratios may be informative of testosterone injection.[30] In our study population, one man with del/del reported the current use of
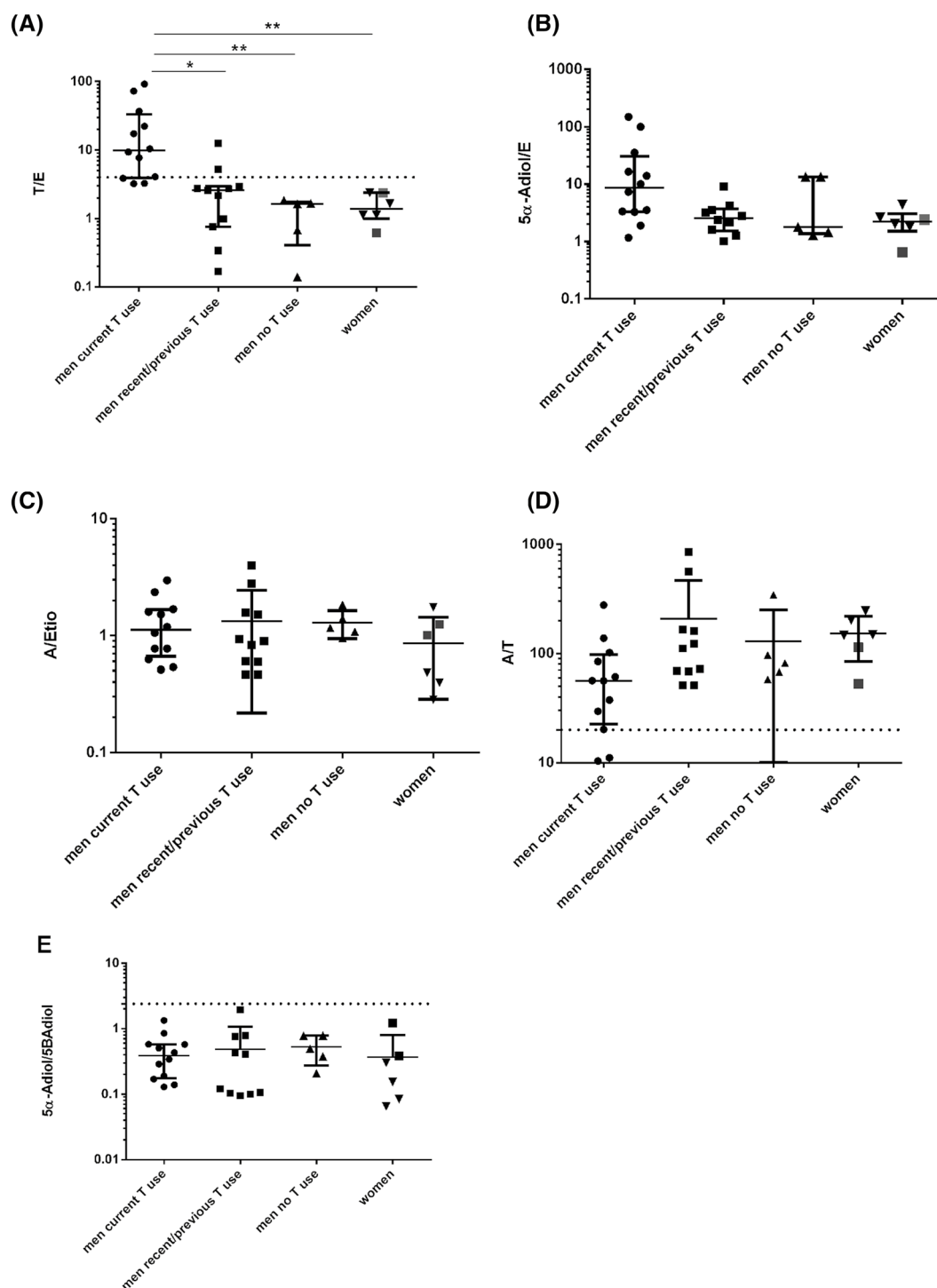
FIGURE 4 ABP biomarkers in AAS using men and women with the results presented as median with interquartile range. Men are grouped in three panels; current testosterone use and recent/previous use (within the last 2–12 months) and no testosterone use within the last year. Women with a current testosterone use are denoted by squares. Dotted lines refer to cut-off ratios, indicative of a suspicious result according to WADA criteria. Kruskal Wallis followed by Dunn's comparison test was used *$P < 0.05$, **$P < 0.01$

testosterone injections and he displayed the lowest T/E ratio (4.1) among the current users which is in agreement with previous findings.[31]

The high circulatory total testosterone level of 9.92 nmol/L observed in the female participant using solely testosterone gel (70 mg/week) is in the same range as that found after 8 weeks of daily administration of 10 mg topical testosterone in healthy women. Notably, such an increase in testosterone is associated with performance enhancing effects which further augments the need to detect transdermal use of testosterone in

TABLE 2 Median values (range) of clinical serum biomarkers in men with a current, recent or previous AAS use

Clinical biomarkers males	Current users (n = 16) (≤ 2 months)	Recent users (n = 9) (2–6 months)	Previous users (n = 5) (6–12 months)	Reference value	P-value
HB, g/dL	16.35 (13.30–19.00)	15.10 (13.90–17.70)	15.30 (14.60–16.10)	13.4–17	0.07
HCT %	49.10 (39.80–57.60)	44.80 (42.70–52.30)	44.60 (44.00–47.50)	39–50	0.07
RET %	1.46 (0.50–2.15)	1.20 (0.80–2.07)	1.19 (0.97–1.71)	NA	0.71
Chol, mmol/L	3.95 (2.50–6.60)	3.90 (3.20–5.90)	4.20 (3.10–6.80)	2.9–7.8[3]	0.71
APO A1 g/L	1.06 (0.55–1.52)	1.27 (0.83–1.9)	1.43 (1.23–1.63)	1.04–2.02	*0.01**
APO B, g/L	0.88 (0.44–1.82)	0.79 (0.57–1.26)	0.62 (0.57–1.43)	0.66–1.33	0.93
HDL, mmol/L	0.90 (0.40–1.60)	1.20 (0.60–1.60)	1.20 (1.10–1.40)	0.8–2.1	0.08
LDL, mmol/L	2.70 (1.10–5.20)	2.30 (1.60–4.00)	1.70 (1.10–4.50)	1.2–5.3[3]	0.87
FSH, E/L	0.14 (0.10–5.00)	1.80 (0.15–5.50)	8.20 (2.30–9.50)	1.5–12	*0.0001* ****
LH, E/L[1]	0.10 (0.10–6.90)[1]	2.60 (0.10–6.60)	6.10 (4.80–9.10)	1.7–8.6	*0.0041* ****
T, nmol/L[2]	25.50 (1.80–50.00)	8.30 (0.80–15.00)	10.00 (6.10–20.00)	6.7–29[3]	*0.01**
SHBG, nmol/L	19.00 (5.400–50.00)	29.00 (12.00–49.00)	27.00 (20.00–38.00)	18–77 [3]	0.36

[1]0.10 minimum quantification level.
[2]50 nmol/L maximum quantification level
[3]Age dependent
HB, hemoglobin; HCT, hematocrit; RET, reticulocytes; Chol, cholesterol; APO A1, apolipo protein A1; APO B, apolipo protein B; HDL, high-density lipoprotein cholesterol; LDL, low-density lipoprotein cholesterol; FSH, follicle stimulating hormone; LH, luteinizing hormone; T, testosterone; SHBG, sex hormone-binding globulin.

TABLE 3 Individual values of different serum biomarkers in women

Clinical biomarkers females	F 2	F 3 [2]	F 5 [3]	F 10	F 22 [4]	F 41	Reference value
HB, g/dL	14.40	14.70	15.20	14.10	14.10	15.4	11.7–15.3
HCT	43.0	44.1	45.5	43.3	42.7	47.5	35–46
Ret%	2.74	1.22	1.44	1.04	1.08	1.28	NA
Chol, mmol/L	4.2	4.3	3.5	5.1	4.1	5.0	2.9–7.8 [5]
APO A1, g/L	0.98	0.70	0.67	1.32	0.68	0.99	1.08–2.25
APO B, g/L	1.01	1.68	1.22	0.72	1.36	1.14	0.60–1.17
HDL, mmol/L	0.8	1.7	1.1	0.6	1.6	0.9	1.0–2.7
LDL, mmol/L	2.9	2.0	1.6	4.3	2.0	3.5	1.2–5.3[5]
FSH, E/L	4.9	1.3	6.9	43	5.0	8.3	1–22 26–135 (post menopause)
LH, E/L [1]	11	1.9	13	44	3.3	9.3	1–96
T, nmol/L (RIA)	1.4	28	3.6	0.4	4.5	0.9	0.1–1.7 [5]
T, nmol/L (LC–MS/MS)	0.24	9.92	1.73	< 0.1	< 0.1	0.29	0.1–1.7 [5]
SHBG, nmol/L	6.7	41	41	18	46	35	32–128 [5]
DHTS, ng/mL	184	560	275	122	237	19	NA

[1]0.10 minimum quantification level.
[2]Current T use (only testosterone-gel).
[3]Current use (testosterone-gel and synthetic steroids were reported and confirmed).
[4]Previous testosterone use.
[5]Age dependent.
HB, hemoglobin; HCT, hematocrit; RET, reticulocytes; Chol, cholesterol; APO A1, apolipo protein A1; APO B, apolipo protein B; HDL, high-density lipoprotein cholesterol; LDL, low-density lipoprotein cholesterol; FSH, follicle stimulating hormone; LH, luteinizing hormone; T, testosterone; SHBG, sex hormone-binding globulin; DHTS, dihydrotestosterone sulfate.

women.[32] Recently it has been discussed to include serum steroid biomarkers in future ABP, as dihydrotestosterone may improve the sensitivity of the ABP to detect the use of topical testosterone in men.[27,33] In the women, in addition to high testosterone levels, DHTS levels were nominally higher in the two testosterone gel using women compared with the other four women. Dihydrotestosterone is mainly found as the sulfate conjugate in serum.

In the male participants, serum testosterone concentrations in the current AAS users were higher than in non-testosterone users. After cessation of AAS, the testosterone concentrations normalized and after 6 months none of the men exhibited supra-physiological testosterone concentrations. It can be considered a drawback of this study that testosterone in men only was quantified with RIA. However, the RIA method employed here delivers reliable values and the results of RIA and LC–MS/MS in men do corroborate.[34,35] In women, RIA often overestimates the total testosterone concentration,[36,37] as was also obvious here, and hence LC–MS/MS is superior for analyzing testosterone in women. A limitation though is that the upper range of quantification of total testosterone with RIA is 50 nmol/L, and thus in the male participants injecting testosterone within the last days the absolute concentrations could not be determined. In previous studies, circulatory concentrations higher than 100 nmol/L have been found in some individuals after testosterone administration.[38] In men LH and FSH were normalized within 6–12 months, which is in agreement with other studies performed on AAS users.[31]

Oxandrolone seems to be the most popular AAS among female volunteers, reported by five of six. Oxandrolone was also reported in a large survey to be common among women.[4] After testosterone, trenbolone was the most popular AAS among men in our study population. In studies conducted 10–25 years ago this steroid was not on the top list of AAS.[1,39] Trenbolone and oxandrolone have short half-lives (24 hours) which could be the reason why trenbolone and oxandrolone were detected only in a minority of those who reported the use of these AAS. Another reason might be mislabeling, as only around 40% of confiscated black market AAS are accurately labeled, the percentage being even lower for trenbolone.[40,41]

Drostanolone and nandrolone were the AAS most often detected in participants that *did not* claim such use. This could be due to contamination of other AAS preparations or supplements as shown earlier.[42] Nandrolone may also be detectable in individuals up to a year after cessation due to the long half-life of the metabolite 19-NA.[43] Other studies have also found that self-reported and detected doping agents often do not corroborate for the reasons discussed above.[44,45]

Notably the use of recombinant growth hormone was more frequent in the AAS using women than in the men. Neither of the participants using recGH tested positive with the GH isoform test. We did not conduct the GH2000 biomarker test since in a previous study where recGH doses in the same range were administered, only the GH isoform test could detect recGH.[24] The use of growth hormone releasing peptides/secretagogs was reported in seven participants and surprisingly one was tested positive on ibutamoren (also known as MK-677), even though according to the questionnaire it was administered as droplets 8 weeks earlier. Ibutamoren is the most commonly detected GH releasing secretagog.[46]

As expected, the hematocrit and hemoglobin values were higher in the male participants with a current AAS use compared with those using AAS more than 2 months ago. This is in agreement with previous studies in which the hematocrit (and other hematological parameters) was found to decrease after 6 months of AAS cessation.[47] An elevated hematocrit (50%) may be a risk factor for thrombotic events in AAS users.[48] Notably, none of the AAS using women reached such a high hematocrit value, and the hemoglobin values were within the normal range. This gender difference could simply be due to the lower AAS doses used by women. However, when supra-physiological doses of testosterone were given to transgender men, hematocrits higher than 50% were rarely found.[49] Thus, hematological biomarkers for AAS use may be restricted to men using AAS. Regarding the lipid profile, a difference in ApoA1 between current and previous AAS users was seen. Disturbed lipid values are common for reasons other than using AAS and therefore do not function as a specific AAS biomarker. Moreover, both systolic and diastolic blood pressures observed in our participants were surprisingly high. Even though it is known that AAS users display mild hypertension[48] the blood pressure measured in this study appears higher than in other studies. The reason could be that in other studies 24 hour blood pressures were monitored to avoid white coat syndrome. High blood pressure, disturbed cholesterol profile, and high hematocrit all together increase the risk of cardiovascular diseases.[48]

A limitation with our study is the small number of participants, in particular women. Therefore, it was not possible to make statistical calculations in women, and the gender comparative results should be interpreted with caution. Since doping is illegal in Sweden it is in general difficult to recruit volunteers for studies. Recruiting women is a particular challenge as AAS use is rare in women. Normally repeated test results are included in the athlete biological passport, whereas in our study only single urine and blood samples were taken. However, it would have been difficult to get volunteers for repeated sampling because of the hard to reach population. Another limitation with our study design is that the group division based on "washout" periods may depend on administration routes, different doses, and stacking practice in cycles. Moreover, we have an incomplete history of the participant's use of AAS more than a year ago.

In conclusion, testosterone and oxandrolone are the most popular AAS in Swedish AAS using men and women, respectively. The reported AAS were often not verified in a doping test; nandrolone and drostanolone being the AAS most often detected. The T/E ratio is a valid biomarker for testosterone in men, whereas in women the T/E ratio could not detect the current use of testosterone gel, despite elevated serum testosterone levels. In addition to longitudinally monitoring serum testosterone, dihydrotestosterone(sulfate) may be a putative serum ABP biomarker for detecting testosterone intake in women.

ORCID

Annica Börjesson https://orcid.org/0000-0003-0159-7315
Lena Ekström https://orcid.org/0000-0003-1053-2345

REFERENCES

1. Eklof AC, Thurelius AM, Garle M, Rane A, Sjoqvist F. The anti-doping hot-line, a means to capture the abuse of doping agents in the Swedish society and a new service function in clinical pharmacology. *Eur J Clin Pharmacol*. 2003;59(8–9):571-577.

2. Kanayama G, Pope HG Jr. History and epidemiology of anabolic androgens in athletes and non-athletes. *Mol Cell Endocrinol*. 2018; 464:4-13.

3. Sturmi JE, Diorio DJ. Anabolic agents. *Clin Sports Med*. 1998;17(2): 261-282.

4. Ip EJ, Barnett MJ, Tenerowicz MJ, Kim JA, Wei H, Perry PJ. Women and anabolic steroids: an analysis of a dozen users. *Clin J Sport Med*. 2010;20(6):475-481.

5. Ip EJ, Barnett MJ, Tenerowicz MJ, Perry PJ. The anabolic 500 survey: characteristics of male users versus nonusers of anabolic-androgenic steroids for strength training. *Pharmacotherapy*. 2011;31(8):757-766.

6. Sjoqvist F, Garle M, Rane A. Use of doping agents, particularly anabolic steroids, in sports and society. *Lancet*. 2008;371(9627):1872-1882.

7. Evans NA. Gym and tonic: a profile of 100 male steroid users. *Br J Sports Med*. 1997;31(1):54-58.

8. Anawalt BD. Detection of anabolic androgenic steroid use by elite athletes and by members of the general public. *Mol Cell Endocrinol*. 2018;464:21-27.

9. Sottas PE, Saugy M, Saudan C. Endogenous steroid profiling in the athlete biological passport. *Endocrinol Metab Clin North Am*. 2010;39 (1):59-73. viii-ix

10. World Anti-Doping Agency. TD2019IRMS. 2019. Available from: https://www.wada-ama.org/sites/default/files/td2019irms_final_ eng_clean.pdf

11. Schulze JJ, Lundmark J, Garle M, Skilving I, Ekstrom L, Rane A. Doping test results dependent on genotype of uridine diphospho-glucuronosyl transferase 2B17, the major enzyme for testosterone glucuronidation. *J Clin Endocrinol Metab*. 2008;93(7):2500-2506.

12. Handelsman DJ, Bermon S. Detection of testosterone doping in female athletes. *Drug Test Anal*. 2019;11(10):1566-1571.

13. Ponzetto F, Boccard J, Nicoli R, Kuuranne T, Saugy M, Rudaz S. Steroidomics for highlighting novel serum biomarkers of testosterone doping. *Bioanalysis*. 2019;11(12):1171-1187.

14. Christou GA, Christou MA, Ziberna L, Christou KA. Indirect clinical markers for the detection of anabolic steroid abuse beyond the conventional doping control in athletes. *Eur J Sport Sci*. 2019;19(9):1276-1286.

15. Rane A, Rosen T, Skarberg K, Heine L, Ljungdahl S. Steroids are a growing problem at gyms. *Lakartidningen*. 2013;110(39–40):1741-1746.

16. Garevik N, Borjesson A, Choong E, Ekstrom L, Lehtihet M. Impact of single-dose nandrolone decanoate on gonadotropins, blood lipids and HMG CoA reductase in healthy men. *Andrologia*. 2016;48(5): 595-600.

17. Nieschlag E, Vorona E. Doping with anabolic androgenic steroids (AAS): adverse effects on non-reproductive organs and functions. *Rev Endocr Metab Disord*. 2015;16(3):199-211.

18. Heckathorn DD. Snowball versus respondent-driven sampling. *Sociol Methodol*. 2011;41(1):355-366.

19. World Anti-Doping Agency. TD2016EEAS. 2016. Available from: https://www.wada-ama.org/sites/default/files/resources/files/wada-td2016eaas-eaas-measurement-and-reporting-en.pdf

20. Mullen JE, Thorngren JO, Schulze JJ, et al. Urinary steroid profile in females - the impact of menstrual cycle and emergency contraceptives. *Drug Test Anal*. 2017;9(7):1034-1042.

21. World Anti-Doping Agency. TD2018MRPL. 2018. Available from: https://www.wada-ama.org/sites/default/files/resources/files/ td2018mrpl_v1_finaleng.pdf

22. World Anti-Doping Agency. TD2018DL. 2018. Available from: https://www.wada-ama.org/sites/default/files/resources/files/ td2018dl_v1_en.pdf

23. Elmongy H, Masquelier M, Ericsson M. Development and validation of a UHPLC-HRMS method for the simultaneous determination of the endogenous anabolic androgenic steroids in human serum. *J Chromatogr A*. 2019;460686.

24. Lehtihet M, Bhuiyan H, Dalby A, Ericsson M, Ekstrom L. Longitudinally monitoring of P-III-NP, IGF-I, and GH-2000 score increases the probability of detecting two weeks' administration of low-dose recombinant growth hormone compared to GH-2000 decision limit and GH isoform test and micro RNA markers. *Drug Test Anal*. 2019;11(3):411-421.

25. World Anti-Doping Agency. Prohibited list. 2019. Available from: https://www.wada-ama.org/sites/default/files/wada_2019_english_ prohibited_list.pdf

26. Miller GD, Nair V, Morrison MS, Summers M, Willick SE, Eichner D. Intranasal delivery of Natesto(R) testosterone gel and its effects on doping markers. *Drug Test Anal*. 2016;8(11–12):1197-1203.

27. Mullen J, Borjesson A, Hopcraft O, et al. Sensitivity of doping biomarkers after administration of a single dose testosterone gel. *Drug Test Anal*. 2018;10(5):839-848.

28. Choong E, Schulze JJ, Ericsson M, Rane A, Ekstrom L. Discordant genotyping results using DNA isolated from anti-doping control urine samples. *Drug Test Anal*. 2017;9(7):994-1000.

29. Okano M, Ueda T, Nishitani Y, Kano H, Ikekita A, Kageyama S. UDP-glucuronosyltransferase 2B17 genotyping in Japanese athletes and evaluation of the current sports drug testing for detecting testosterone misuse. *Drug Test Anal*. 2013;5(3):166-181.

30. Strahm E, Mullen JE, Garevik N, et al. Dose-dependent testosterone sensitivity of the steroidal passport and GC-C-IRMS analysis in relation to the UGT2B17 deletion polymorphism. *Drug Test Anal*. 2015;7 (11–12):1063-1070.

31. Garevik N, Strahm E, Garle M, et al. Long term perturbation of endocrine parameters and cholesterol metabolism after discontinued abuse of anabolic androgenic steroids. *J Steroid Biochem Mol Biol*. 2011;127(3–5):295-300.

32. Hirschberg AL, Elings Knutsson J, Helge T, et al. Effects of moderately increased testosterone concentration on physical performance in young women: a double blind, randomised, placebo controlled study. *Br J Sports Med*. 2019;10(15).

33. Ponzetto F, Mehl F, Boccard J, et al. Longitudinal monitoring of endogenous steroids in human serum by UHPLC-MS/MS as a tool to detect testosterone abuse in sports. *Anal Bioanal Chem*. 2016;408(3): 705-719.

34. Ankarberg-Lindgren C, Norjavaara E. Changes of diurnal rhythm and levels of total and free testosterone secretion from pre to late puberty in boys: testis size of 3 ml is a transition stage to puberty. *Eur J Endocrinol*. 2004;151(6):747-757.

35. Handelsman DJ. Mass spectrometry, immunoassay and valid steroid measurements in reproductive medicine and science. *Hum Reprod*. 2017;32(6):1147-1150.

36. Rezaii T, Gustafsson TP, Axelson M, et al. Circulating androgens and SHBG during the normal menstrual cycle in two ethnic populations. *Scand J Clin Lab Invest*. 2017;77(3):184-189.

37. Taieb J, Mathian B, Millot F, et al. Testosterone measured by 10 immunoassays and by isotope-dilution gas chromatography-mass spectrometry in sera from 116 men, women, and children. *Clin Chem*. 2003;49(8):1381-1395.

38. Garevik N, Rane A, Bjorkhem-Bergman L, Ekstrom L. Effects of different doses of testosterone on gonadotropins, 25-hydroxyvitamin D3, and blood lipids in healthy men. *Subst Abuse Rehabil*. 2014;5: 121-127.

39. Lood Y, Eklund A, Garle M, Ahlner J. Anabolic androgenic steroids in police cases in Sweden 1999-2009. *Forensic Sci Int*. 2012;219(1–3): 199-204.

40. Krug O, Thomas A, Walpurgis K, et al. Identification of black market products and potential doping agents in Germany 2010-2013. *Eur J Clin Pharmacol*. 2014;70(11):1303-1311.

41. Weber C, Krug O, Kamber M, Thevis M. Qualitative and Semiquantitative analysis of doping products seized at the Swiss border. *Subst Use Misuse*. 2017;52(6):742-753.

42. Martello S, Felli M, Chiarotti M. Survey of nutritional supplements for selected illegal anabolic steroids and ephedrine using LC-MS/MS and GC-MS methods, respectively. *Food Addit Contam*. 2007;24(3): 258-265.

43. Bagchus WM, Smeets JM, Verheul HA, De Jager-Van Der Veen SM, Port A, Geurts TB. Pharmacokinetic evaluation of three different intramuscular doses of nandrolone decanoate: analysis of serum and urine samples in healthy men. *J Clin Endocrinol Metab*. 2005;90(5): 2624-2630.

44. Borjesson A, Garevik N, Dahl ML, Rane A, Ekstrom L. Recruitment to doping and help-seeking behavior of eight female AAS users. *Subst Abuse Treat Prev Policy*. 2016;11:1-6.

45. Pope HG, Katz DL Jr. Psychiatric and medical effects of anabolic-androgenic steroid use. A controlled study of 160 athletes. *Arch Gen Psychiatry*. 1994;51(5):375-382.

46. World Anti-Doping Agency. Anti-Doping Testing Figures by Laboratory. 2017. Available from: https://www.wada-ama.org/sites/default/files/resources/files/2017_anti-doping_testing_figures_en_0.pdf

47. Mullen J, Gårevik N, Schulze J, Rane A, Bergman L, Ekström L. Perturbation of the hematopoietic profile by anabolic androgenic steroids. *J Hormones*. 2014;2014:510257. https://doi.org/10.1155/2014/510257

48. Chang S, Munster AB, Gram J, Sidelmann JJ. Anabolic androgenic steroid abuse: the effects on thrombosis risk, coagulation, and fibrinolysis. *Semin Thromb Hemost*. 2018;44(8):734-746.

49. Defreyne J, Vantomme B, Van Caenegem E, et al. Prospective evaluation of hematocrit in gender-affirming hormone treatment: results from European network for the investigation of gender incongruence. *Andrology*. 2018;6(3):446-454.

SUPPORTING INFORMATION

Additional supporting information may be found online in the Supporting Information section at the end of this article.

WILEY

WILEY

Account Manager: Hagen Reichhoff

Editor: Dr. Christina Poggel, *Wiley Analytical Science*

Imprint